ACS APPLIED MATERIALS & INTERFACES

www.acsami.org

Forum Article

Reviews on Machine Learning Approaches for Process Optimization in Noncontact Direct Ink Writing

Haining Zhang and Seung Ki Moon*

Cite This: https://doi.org/10.1021/acsami.1c04544

Read Online

ACCESS | Metrics & More | Article Recommendations

ABSTRACT: Recently, machine learning has gained considerable attention in noncontact direct ink writing because of its novel process modeling and optimization techniques. Unlike conventional fabrication approaches, noncontact direct ink writing is an emerging 3D printing technology for directly fabricating low-cost and customized device applications. Despite possessing many advantages, the achieved electrical performance of produced microelectronics is still limited by the printing quality of the noncontact ink writing process. Therefore, there has been increasing interest in the machine learning for process optimization in the noncontact direct ink writing. Compared with traditional approaches, despite machine learning-based strategies having great potential for efficient process optimization, they are still limited to optimize a specific aspect of the printing process in the noncontact direct ink writing. Therefore, a systematic process optimization approach that integrates the advantages of state-of-the-art machine learning techniques is in demand to fully optimize the overall printing quality. In this paper, we systematically discuss the printing principles, key influencing factors, and main limitations of the noncontact direct ink writing technologies based on inkjet printing (IJP) and aerosol jet printing (AJP). The requirements for process optimization of the noncontact direct ink writing are classified into four main aspects. Then, traditional methods and the state-of-the-art machine learning-based strategies adopted in IJP and AJP for process optimization are reviewed and compared with pros and cons. Finally, to further develop a systematic machine learning approach for the process optimization, we highlight the major limitations, challenges, and future directions of the current machine learning applications.

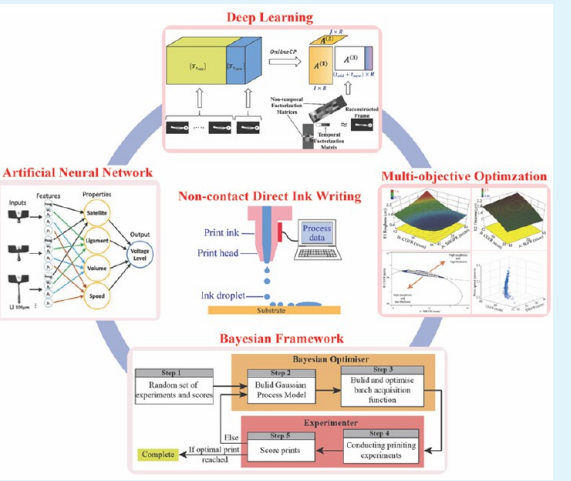

KEYWORDS: *noncontact direct ink writing, printed electronics, aerosol jet printing, inkjet printing, machine learning, process optimization*

1. INTRODUCTION

Recently, machine learning has gained considerable attention in noncontact direct ink writing because of its novel process modeling and optimization techniques. Unlike contact direct printing as shown in Table 1, the noncontact direct ink writing is an emerging printed electronics technology in an electronic manufacturing industry.[1−7] Because of the capability of printing with higher resolution and producing less chemical waste,[8−14] it has been widely adopted for fabrication of flexible, customized microelectronics, such as transistors,[15−18] energy harvesting/storage devices,[19−22] radio frequency identification tags (RFID),[23−26] and sensors with various functions.[27−36] However, as the achieved electrical performance of produced microelectronics is still limited by the printing quality of the noncontact ink writing process,[37−40] the machine learning for process optimization in noncontact direct ink writing has received increasing interest.

Moreover, as shown in Table 1, despite there being solvent-free noncontact direct printing techniques, including organic vapor jet printing (OVJP) and laser direct writing (LDW), ink-based noncontact direct writing techniques are more receivable in the printed electronics industry because of relatively higher throughput and fewer substrate limitations.[6,86,87] Figure 1 shows the basic working principles of traditional fabrication process and direct printing process for fabricating electronics. And the comparison between classical noncontact direct printing technologies is discussed in the next section.

Although possessing many advantages, there is an urgent need to optimize the printing quality of the noncontact direct ink writing. Because of the restriction of the adopted ink properties,[89−93] such as ink viscosity, density, and surface

Special Issue: Artificial Intelligence/Machine Learning for Design and Development of Applied Materials

Received: March 10, 2021
Accepted: May 17, 2021

Table 1. Main Types of Direct Printing Methods for Printed Electronics

printing methods	fabrication types	material types	ref
screen printing	contact printing	ink based	16,21,41−43
gravure printing	contact printing	ink based	17,44−47
soft lithography	contact printing	ink based	48−52
offset printing	contact printing	ink based	53−57
flexographic printing	contact printing	ink based	58−61
fused deposition modeling	contact printing	filament based	36,62−64
aerosol jet printing	noncontact ink writing	ink based	37,40,65−72
inkjet printing	noncontact ink writing	ink based	38,39,71−74
organic vapor jet printing	noncontact printing	vapor based	6,75−78
laser direct writing	noncontact printing	nanoparticle based	29,30,79,80
hybrid printing	contact/noncontact printing	multimaterial based	7,81−85

tension, a conductive line can be produced with high overspray or discontinuity, which will induce the risk of open/short circuiting of printed electronic components. Even a conductive line is produced with excellent continuity and low overspray, the high edge roughness will significantly reduce the uniformity of the printed line resistance,[94−97] which is detrimental to resistive sensors. Moreover, if the conductive line produced insufficient thickness, the postprinting process will cause voids and concaves to the line centers because of the coffee-ring effect,[98−101] which will significantly reduce the electrical performance of the printed patterns. Hence, it is necessary to further optimize the printed line morphology (line thickness and edge roughness) simultaneously to improve the electrical performance. Besides line morphology optimization, printing high resolution, and small gap patterns on a substrate have been given more attention in the noncontact ink writing technologies.[102−105] In this case, there is a need to achieve the high controllability of the printed line width. However, because of the variations of many influencing factors during printing,[106−108] including solvent evaporation, temperature fluctuations, and ink properties, the printing process has an uncontrollable tendency to drift, which will invalidate the existing optimal parameter settings, and deteriorate the optimized electrical performance of the fabricated electronic components. Therefore, to achieve a high electrical performance of the printed electronic components, the requirements for printing process optimization can be classified into four main aspects: (1) ink printability, (2) line morphology optimization, (3) line width controllability, and (4) process drift calibration. As the ink printability mainly refers to the capability to print lines with less overspray or satellite droplets using a noncontact ink writing technology, it can be quantified by the average distance between the printed line edges and the discrete overspray spots (or satellite droplets), and higher average distance demonstrates lower ink printability. Besides the ink printability, as a high level of edge roughness and insufficient line thickness will greatly reduce the performance of produced electronic devices, it is important to further optimize the printed line morphology by minimizing the line edge roughness while maximizing line thickness. On the other hand, line width controllability refers to the ability to print customized line width using the noncontact ink writing technology, which can be evaluated by the ratio of the printed line width to the target line width. Moreover, because of the impact of many changing factors during printing, the noncontact ink writing process tends to drift over time. Therefore, process drift calibration aims to reduce the impact of the changing factors, and the variations in the printed geometrical (electrical) properties with respect to time can be used to quantify the influence of process drift on printing quality.

Despite the printing process being affected by various factors, such as ink properties, substrate properties, and random variations, the process parameters are preferred to the process optimization of the noncontact ink writing technology, because the parameters have a great impact on

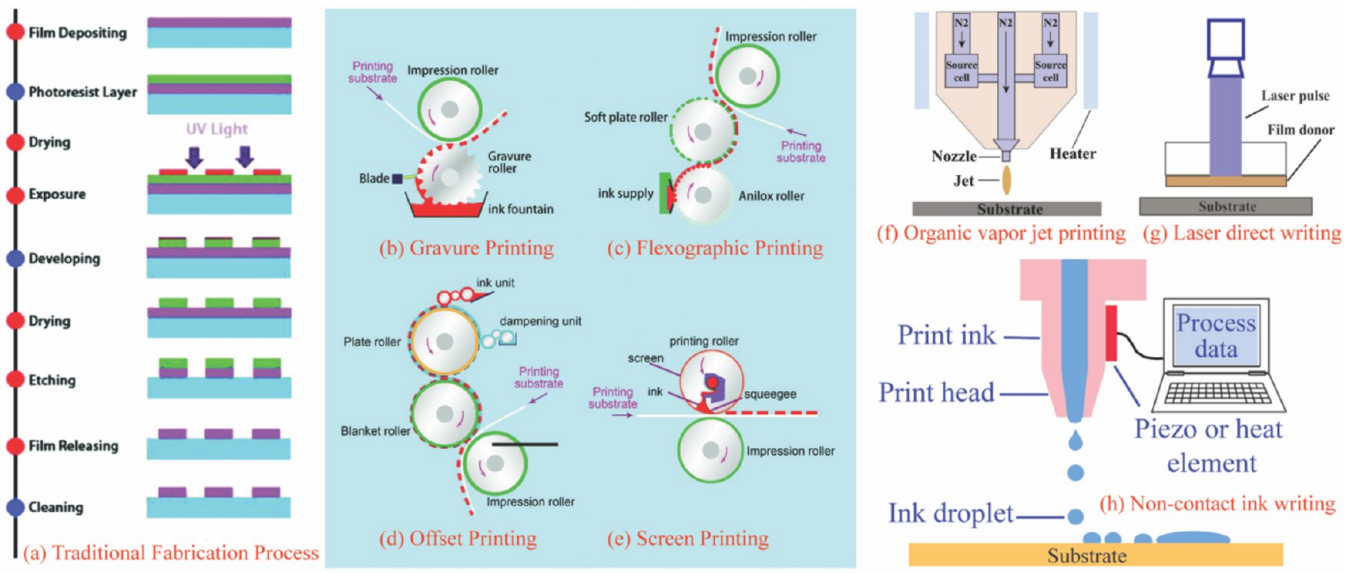

Figure 1. Comparison between traditional fabrication process and direct printing process. (a) Traditional fabrication process, (b−e) contact direct printing process. Reprinted with permission from ref 88. Copyright 2017 Royal Society of Chemistry. (f−g) Solvent-free noncontact direct printing process. (h) Ink-based noncontact direct writing process.

https://doi.org/10.1021/acsami.1c04544
ACS Appl. Mater. Interfaces XXXX, XXX, XXX−XXX

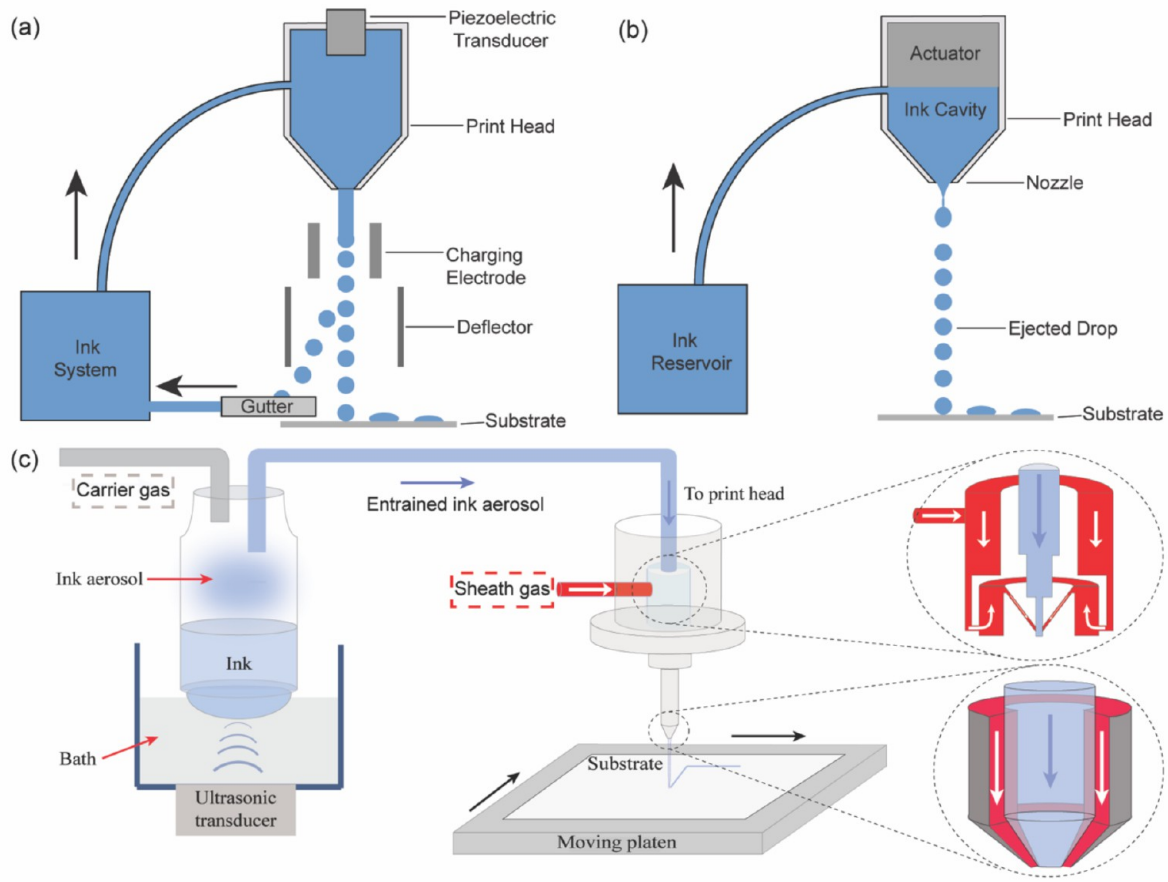

Figure 2. Working principles of (a) continuous inkjet printing, (b) drop-on-demand inkjet printing, and (c) aerosol jet printing using an ultrasonic atomizer. Reprinted with permission from ref 116. Copyright 2019 Springer.

the printed line characteristics and are adjustable during printing.[109−112] However, as determining the exactly cause-effect correlations of the printing process remains a challenge, many designers adopt empirical operational approaches to manually optimize the printing process, which will be imprecise and inefficient due to the insufficient exploration of a design space and lack of quantitative modeling. Despite computational fluid dynamics (CFD) models based on specific printing systems and model simplifications having been proposed for quantitative analysis of the noncontact ink writing process,[113−115] it will be difficult to propose a CFD model with high accuracy because of the limited computational resource, which will hinder its applications in real-time printing process optimization. In this case, machine learning based strategies are preferred to efficient process optimization by introducing new process modeling and optimization methods. However, because of the impact of many changing factors during printing, the developed stationary machine learning strategies for the process optimization may not suffice for printing quality assurance. Therefore, it is necessary to further integrate the advantages of in situ monitoring and closed-loop control for in-process diagnosis and online optimization, which will be helpful to ensure process stability and optimization efficiency during printing.

In this paper, we systematically discuss the printing principles, key influencing factors, and main limitations of the noncontact direct ink writing technologies based on inkjet printing (IJP) and aerosol jet printing (AJP). Requirements of the process optimization of noncontact direct ink writing are classified into four main aspects. Then, traditional methods and the state-of-the-art machine learning-based techniques adopted in IJP and AJP for process optimization are reviewed and compared with pros and cons. Finally, to further develop a systematic machine learning approach for the process optimization, we also highlight the major limitations, challenges and future directions of the current machine learning applications.

This paper is organized as follows: Section 2 describes the current state of the art of noncontact direct ink writing technologies. Section 3 discusses traditional printing quality optimization approaches in the noncontact direct writing process. Section 4 reviews state-of-the-art machine learning-based techniques for process optimization in noncontact ink writing. In Section 5, the paper is concluded by providing limitations, challenges, and future directions for the current machine learning applications to further enrich the noncontact direct ink writing technology.

2. CURRENT STATE OF THE ART OF NONCONTACT DIRECT INK WRITING TECHNOLOGIES

2.1. Overview of Noncontact Direct Ink Writing Technologies for Functional Applications. *2.1.1. Noncontact Direct Ink Writing Process.* As the basic functional materials of printed electronics are usually nanoparticles, such as carbon nanotubes, metal nanoparticles and conductive polymers, special solvents are required to formulate different functional inks for noncontact direct ink writing technologies. As shown in Figure 2, IJP and AJP are two representative

https://doi.org/10.1021/acsami.1c04544
ACS Appl. Mater. Interfaces XXXX, XXX, XXX−XXX

Table 2. Technical Specifications of Classical Noncontact Direct Printing Techniques[6,113,116,120]

printing methods	ink viscosity (cP)	feature size (μm)	process speed (m/min)	advantages	disadvantages
IJP	10−20	>30	15−500	print on flexible substrates	nozzle clogging
				print with multimaterials	coffee-ring effect
				low chemical wastes	not suitable for nonplanar surface
				low cross-contamination	constraints of ink formulation
AJP	1−2500	10−200	up to 12	print on flexible substrates	require additional supplying systems
				print on nonplanar surface	constraints of ink formulation
				high-resolution printing	coffee-ring effect
				elimination of nozzle clogging	
OVJP		<25	<4 × 10^{-6}	free from solvent	not suitable for flexible substrates
				print with multimaterials	relatively low print speed
				low chemical wastes	require additional supplying systems
LDW		<20	depending on laser's speed	no requirement of vacuum	not suitable for flexible substrates
				print with multimaterials	laser irradiation can damage patterns
				low chemical wastes	high-power laser consumption

solvent-based noncontact direct ink writing technologies that have been adopted to produce electrical and electronic devices in a broad variety of applications. On the basis of the principles of droplet formation and ejection, IJP can be divided into continuous inkjet (CIJ) printing system and drop-on-demand (DoD) printing system.[117−119] For a CIJ printing system as shown in Figure 2a, a continuous ink flow is broken up into droplets uniformly by the controlled thermal or piezoelectric disturbance. As the generated droplets will pass through an electric field, some ink droplets will be charged and captured for reuse, whereas the remaining uncharged droplets will land on a substrate as printed patterns. Different from the CIJ printing system, a single droplet of a DoD printing system (Figure 2b) is generated by a rapid change in the cavity volume. The generated droplets are then ejected and printed onto a substrate because of the applied momentum. Compared with the CIJ system, as the DoD system has the capability of producing less waste and printing with higher resolution, it is widely adopted for printing electronics and will be discussed in this paper. Compared with IJP, AJP is one of the most recent techniques that is commercially available in various research fields and the printed electronic industry. Figure 2c demonstrates the basic printing principles of AJP based on an ultrasonic atomizer. In this technique, the formulated nanoparticle ink is atomized into ink aerosol by a pneumatic or ultrasonic atomizer. The generated ink aerosol is entrained to the nozzle by a carrier gas flow and then enwrapped cylindrically by a sheath gas flow in the nozzle tip. Finally, as a highly collimated aerosol droplets will print onto the moving substrate with high velocity, a fine conductive line with high density will be produced on the substrate.

2.1.2. Comparison between Classical Noncontact Direct Printing Technologies. The comparison of basic technical specifications between classical noncontact direct printing techniques with advantages and disadvantages is shown in Table 2. Because of the capability of printing on flexible substrates with a high process speed, IJP has been adopted as a representative noncontact direct ink writing technique for printing electronics. Despite possessing a relatively lower process speed, AJP is currently the most receivable noncontact direct ink writing technique for producing sensors and electronic patterns because of its capability of printing on nonplanar surface with higher resolution and less limitations on ink viscosity. Although the solvent-free noncontact direct printing technologies such as OVJP and LDW can eliminate solvent incompatibility, the coffee-ring effect, and other issues restricting noncontact direct ink writing, they are rarely used in large-scale electronic device manufacturing because of their relatively lower throughput and rigid substrate requirements. Therefore, IJP and AJP are preferred in the printed electronic industry and will be systematically discussed in this paper.

2.2. Current State of the Art of Noncontact Direct Ink Writing Process. *2.2.1. Analysis of the Noncontact Direct Ink Writing Process.* To achieve printing quality optimization and ensure high controllability of the printed line features, it is important to systematically analyze the manufacturing process of noncontact direct ink writing and identify the cause−effect correlation between impact factors and the printed line features accurately. As shown in Figure 3, the manufacturing process of the noncontact ink writing consists of three phases: (1) preprinting, (2) the printing process, and (3) postprinting.[109,111] Table 3 lists the main influencing factors of each phase. It can be seen that the preprinting and printing process phases can influence the printed line morphology directly, whereas the postprinting phase will influence the uniformity of the cross-sectional profile because of the coffee-ring effect. As the printed line morphology has a direct impact on the cross-sectional profile, the real-time optimization and control of the printed line morphology are considered to be the main challenges in the manufacturing process.[113,121] Moreover, as the printed line features are the outcomes of interaction between printing process parameters and preprinting factors, it is important to identify the relationship between key adjustable process parameters and the printed line features accurately,

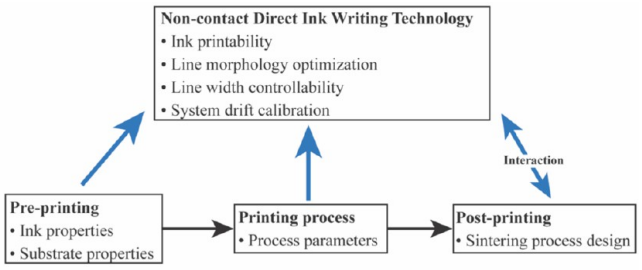

Figure 3. Correlations between different fabrication stages of noncontact direct ink writing technology.

https://doi.org/10.1021/acsami.1c04544
ACS Appl. Mater. Interfaces XXXX, XXX, XXX−XXX

Table 3. Main Influencing Factors of Noncontact Direct Ink Writing Techniques

categories	main influencing factors
preprinting factors[122−125]	ink properties: ink concentration, ink density, ink viscosity, particle size, surface tension
	substrate properties: substrate temperature, surface wettability, surface roughness, contact angle
printing process parameters[111,126−134]	IJP: voltage, droplet spacing, waveform, printing height, jetting delay, nozzle size
	AJP: sheath gas flow rate, carrier gas flow rate, atomizer current, process speed, nozzle size, working distance
postprinting factors[135−140]	oven: sintering time, sintering temperature, temperature gradient, sintering cycles
	laser: laser power, scanning speed, scanning spacing, scanning runs
	UV: UV spectrum, UV power, conveyor speed, exposure times

which will be beneficial to high printed line quality and controllability of noncontact direct ink writing process.

2.2.2. Current Limitations of Noncontact Ink Writing Process. In recent years, despite noncontact ink writing technologies having demonstrated remarkable progress in fine-line patterning and multilayering of microelectronics, ink printability still poses a challenge for further miniaturization of microelectronic devices. The ink printability is primarily affected by fluid properties, and the critical properties of printing ink are ink viscosity, surface tension, and ink density.[141−147] For example, as shown in Figure 4a−f, because of the restriction of ink properties used in IJP, a conductive line can be printed with high splashing or satellite droplets, which is not conductive to miniaturization of microelectronic devices. Despite AJP having the capability of processing high viscosity ink (1−2500 cP), the conductive line can be produced with high overspray or discontinuity as shown in Figure 4g−i, due to the complex interaction between different process parameters. Thus, it is important to analyze the impact of physical properties and main process parameters on characteristics of the ink printability, and the printable range of ink properties and operating conditions can be determined to ensure the printability of noncontact ink writing technologies.

Even an optimal printable range can be identified for a noncontact direct ink writing technology, the produced line features may still suffer from certain defects: a high level of edge roughness and insufficient line thickness will significantly affect the performance of produced electronic devices.[96,97,110] As shown in Figure 5a−h, conductive lines are printed with high edge roughness because of the adopted inappropriate process parameters, which is detrimental to the uniformity of the printed line resistance. On the other hand, because of the coffee-ring effect (Figure 6), the deposited functional ink has a tendency to distribute nonuniformly from the middle of line to the line edges during the postprinting process.[98−101] In this case, voids and concaves will be induced to the line centers due to an insufficient line thickness (Figure 5i−j), which will significantly reduce the conductivity of printed components. Hence, it is crucial to increase the printed line thickness and reduce line edge roughness during printing simultaneously.

As many advanced electronic designs are used in the mobile industry and the aerospace industry requires device applications such as sensors, integrated circuits, and antennae to be printed onto narrow surfaces, printing high resolution and small gap patterns on a substrate have been given more attention in noncontact ink writing technology.[153−155] For example, the fabrication of narrow electrodes can effectively increase the active light receiving surface area of solar cells to improve power generation efficiency.[156,157] However, as the feature size and resolution of the printed lines is very sensitive to process parameters, the low controllability of the printing process will induce inhomogeneous printed line morphology and relative coarse resolution of deposited patterns, which will

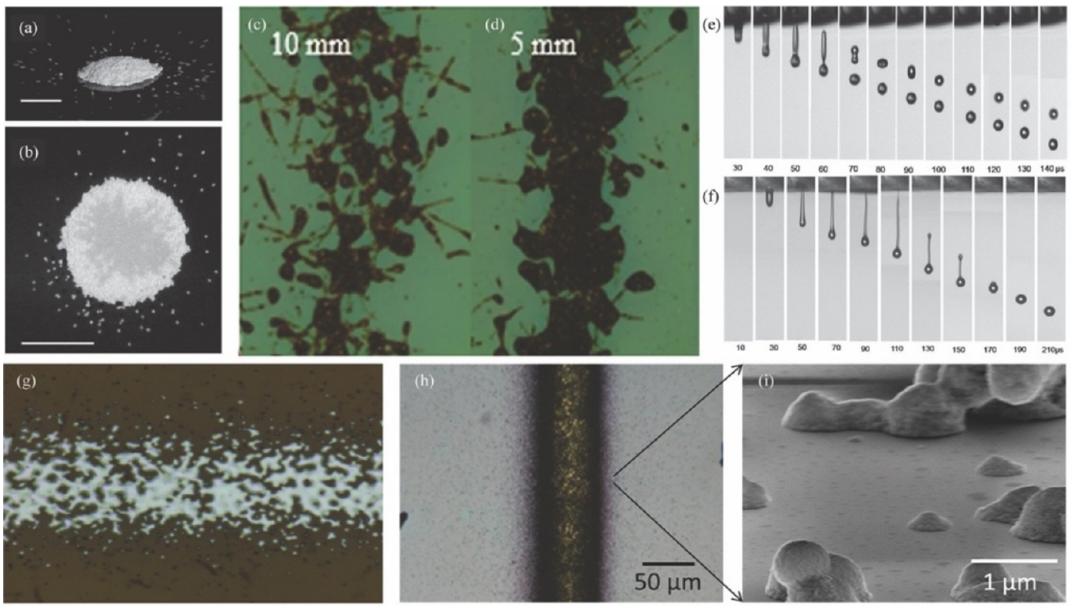

Figure 4. Limitations of noncontact direct ink writing technology in ink printability. (a, b) Splashing drops of IJP. Reprinted with permission from ref 148. Copyright 2013 American Physical Society. (c, d) High splashing lines of IJP. Reprinted with permission from ref 149. Copyright 2019 Springer Nature. (e, f) Lines with satellites of IJP. Reprinted with permission from ref 150. Copyright 2009 American Chemical Society. (g) Discontinuous line of AJP. (h, i) High overspray line of AJP. Reprinted with permission from ref 132. Copyright 2013 American Chemical Society.

https://doi.org/10.1021/acsami.1c04544
ACS Appl. Mater. Interfaces XXXX, XXX, XXX−XXX

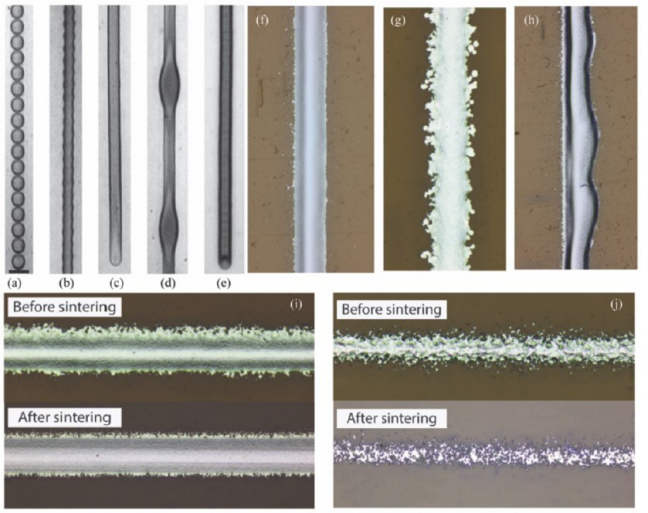

Figure 5. Limitations of noncontact direct ink writing technology in printed line features. (a–e) Printed line morphology with different edge roughness based on IJP. Reprinted with permission from ref 100. Copyright 2008 American Chemical Society. (f–h) Printed line morphology with different edge roughness based on AJP, (i, j) comparison between lines with sufficient and insufficient thickness after the postprinting process. Reprinted with permission from ref 151. Copyright 2020 Elsevier.

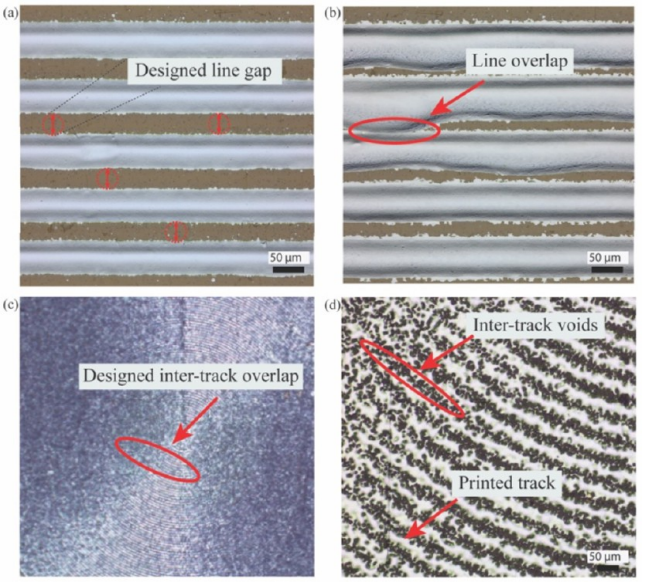

Figure 7. Limitations of noncontact direct ink writing technology in line width controllability. (a) Narrowly spaced lines with controlled line width. (b) Overlap printing due to the low controllability of line width. (c) Ideally printed surface morphology with controlled intertrack overlap. (d) Induced intertrack voids in the printed surface morphology due to low controllability of intertrack overlap.

prevent the noncontact ink writing technologies from being widely applied to various advanced applications. As shown in Figure 7a, b, because of the low controllability of the printed line morphology, the narrowly spaced circuits may overlap, which will cause a cross-finger shorting in the fabricated electronic components.[158] On the contrary, as shown in Figure 7c, d, inaccurate control of printed track width results in unnecessary intertrack voids, which leads to open circuits in

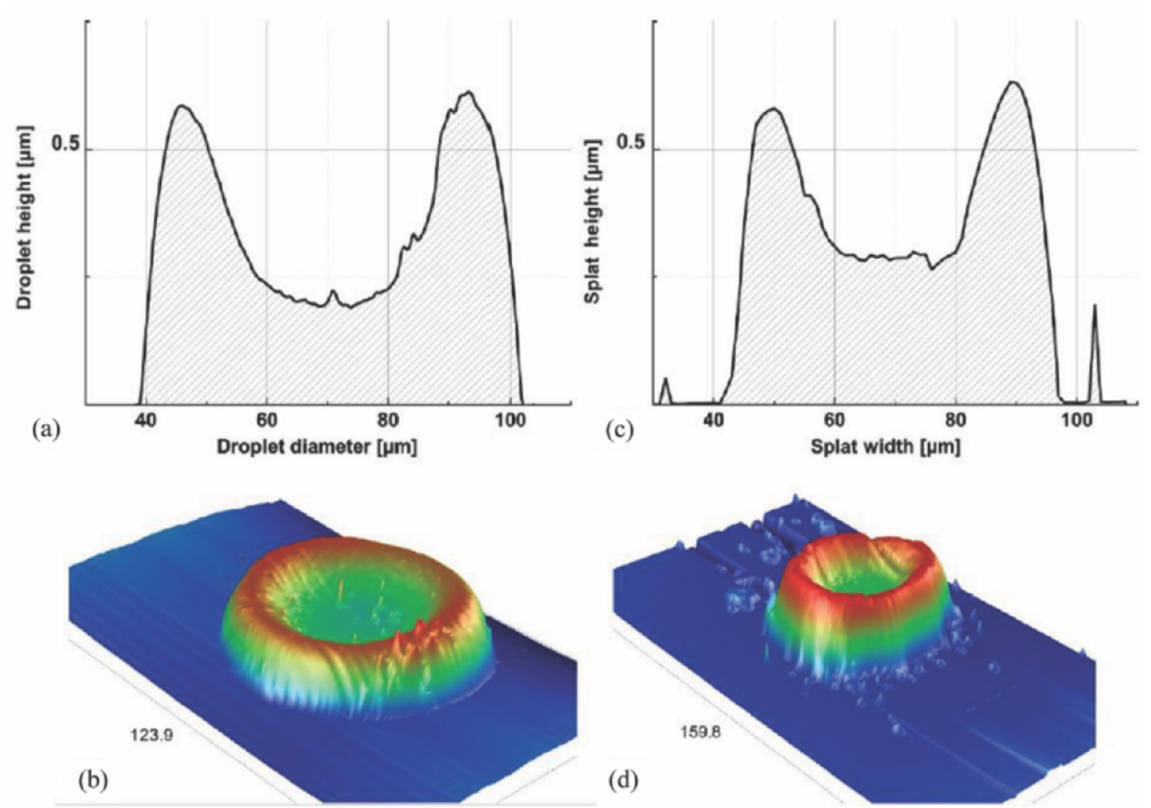

Figure 6. Coffee-ring effect induced 2D and 3D profile of (a, b) an inkjet-printed droplet and (c, d) an aerosol jet-printed droplet. Reprinted with permission from ref 152. Copyright 2015 American Chemical Society.

https://doi.org/10.1021/acsami.1c04544
ACS Appl. Mater. Interfaces XXXX, XXX, XXX–XXX

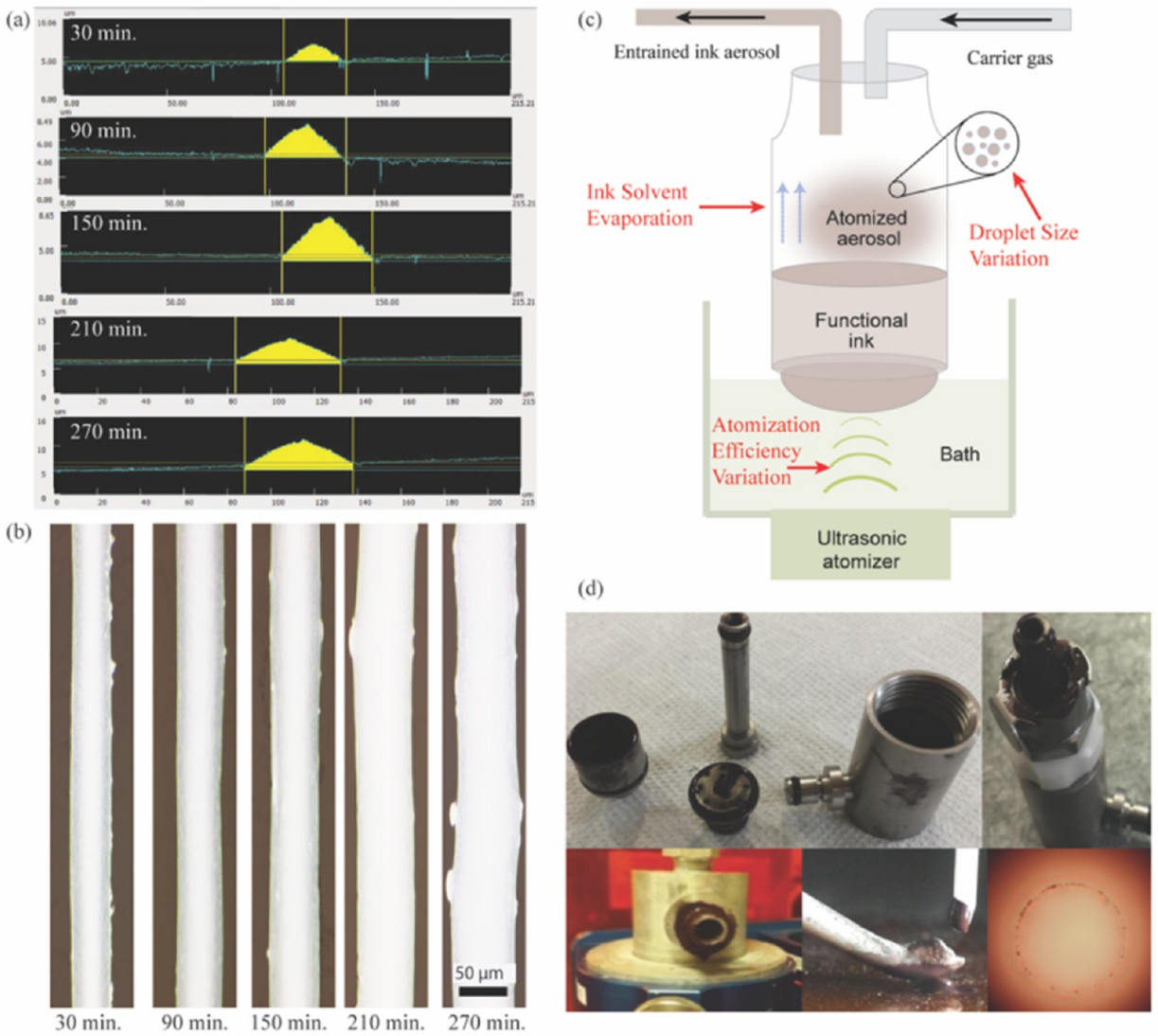

Figure 8. Limitations of noncontact direct ink writing technology in process drift. (a) Process drift in printed line thickness with time. (b) Process drift in printed line width with time. (c) Main causes of process drift in AJP. (d) Ink accumulation in the deposition head. Reprinted with permission from ref 165. Copyright 2015 RIT Scholar Works.

the designed surface morphology. Therefore, the high controllability of line width is of primary importance for advanced applications of the noncontact ink writing technologies.

Despite noncontact ink writing technology having been successfully utilized in printed electronics industry and various research areas, its widespread adoption at a large industry scale level for manufacturing and fabrication is hindered by issues in reproducibility and process consistency. The poor reproducibility and process consistency of a noncontact ink writing system can be attributed to process drift, which means the deposition rate of the noncontact ink writing process will vary significantly, even over a relatively short duration of printing.[106,159,160] Therefore, as shown in Figure 8a, b, the printed line morphology[106,161] and the resulting electrical properties[108,162] will greatly change over time, despite the same deposition settings being adopted.

The gradual drift of the noncontact ink writing process arises from two main sources: dynamic effects and secondary effects, both of which can induce irregularities in the process and will have detrimental effects on the printed line morphology.[163,164] As shown in Figure 8c, d, because of solvent evaporation, variations in ink viscosity and accumulation of function ink in the printhead will have a dynamic effect on the gradual drift. Moreover, the variations in ink atomization efficiency, droplet size, and aerodynamics through the printhead will have a secondary effect on process drift. Because of the presence of inevitable process drift, optimal operating windows and empirical process models that developed from experiments offline will be invalid and need further calibration before subsequent printing. However, the vast variability of a design space poses great challenges to efficiently reduce deviations of both geometrical and electrical properties from the target tolerances. Despite researchers being able to periodically discard and refill ink to obtain consistent printed line features with the requisite electrical properties, it will be a major obstacle to widespread industrial adoption because of the presence of severe material waste and confusion of process optimization efforts. Thus, it is important to analyze the impact of process drift on the printed line features and propose an

https://doi.org/10.1021/acsami.1c04544
ACS Appl. Mater. Interfaces XXXX, XXX, XXX−XXX

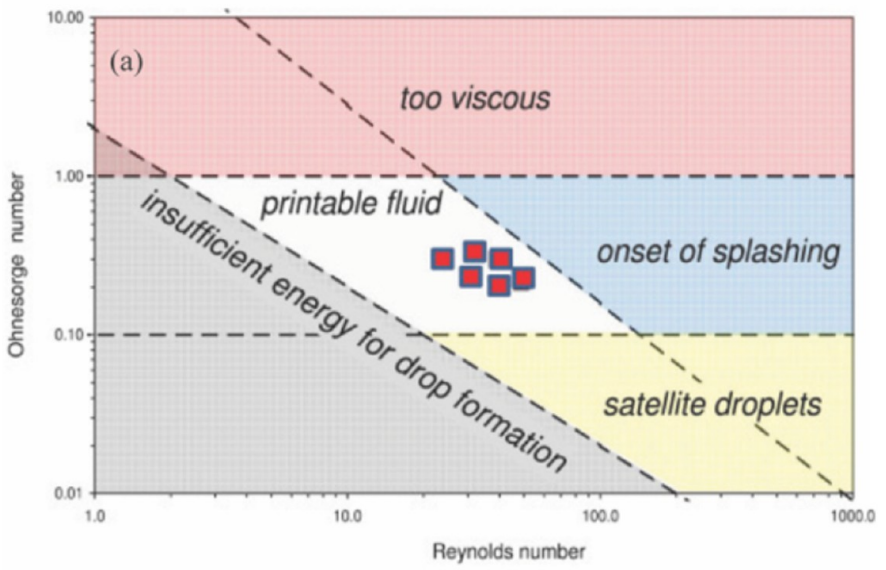

Figure 9. Semiempirical operability window to ensure ink printability of IJP. Reprinted with permission from ref 167. Copyright 2016 Elsevier.

economical calibration approach to compensate the induced process variations and inconsistency during printing.

3. TRADITIONAL PRINTING QUALITY OPTIMIZATION APPROACHES

3.1. Ink Printability. Because of the limitation of ink viscosity, the ink printability of IJP is a primary issue in the application of printed electronics. Therefore, the impact of ink properties on droplet behavior is evaluated by a dimensionless value Z (the reciprocal of the Ohnesorge number),[166] and a semiempirical operability window with respect to fluid properties can be identified to obtain a proper jettability as shown in Figure 9.[167]

$$Z = \frac{(\gamma \rho a)^{1/2}}{\eta} \tag{1}$$

where a, η, γ, and ρ are the tip size, viscosity, surface tension, and density of the fluid, respectively.

However, despite previous research demonstrating that $1 < Z < 10$ can be used as a printable range to ensure the ink printability in most IJP systems,[168] the printability window should be modified to provide the highly nonlinear rheological properties under specific conditions.[169] Therefore, as shown in Table 4, to ensure the printability of low viscosity fluids, we experimentally modified the proposed semiempirical model for stable printing in IJP.

3.2. Printed Line Morphology Optimization. To investigate the influence of droplet coalescence process on the formed line morphology theoretically, Duineveld[181] developed a numerical model to investigate the impact of process speed and droplet distance on the formed line morphology, and a maximum stable liquid bead width was determined to avoid bulging instability. On the basis of the requirements of contact angle and contact line, Davis[182] investigated the stability of overlapping droplets on a flat substrate subject, and the conclusions were further confirmed experimentally.[183] Additionally, a stability model based on the volume conservation theory was proposed[184] to analyze the impact of droplet distance, print speed and contact angle on the boundary of stable liquid beads (Figure 10a). Besides theoretical analysis, Soltman et al.[100] identified the correlations between operating conditions and the coalescence process of produced droplets experimentally, and an empirical process window was determined to improve the printed line quality qualitatively as shown in Figure 10b.

Different from IJP, AJP is not restricted by ink printability because of its capability of printing with high viscosity ink (1−2500 cP). Therefore, various qualitative process windows were developed experimentally to optimize the printed line morphology directly. On the basis of the proposed criteria and the image analysis method, we determined a process window for printing lines with a high level of edge smoothness by Verheecke et al.[111] Moreover, to ensure high printing resolution, Smith et al.[159] evaluated the relationship between printed line quality and influencing factors, and a 2D process

Table 4. Examples of Modified Stable Printing Areas of Different Inks

ref	nozzle diameter (μm)	waveforms	liquid	Z (Oh^{-1})
Jang et al.[170]	50	bipolar	ethylene glycol	1.43−17.32
Jo et al.[171]	50	square	water/glycol mixture	3.03−41.67
Seerden et al.[172]	35		wax-based Al suspension	2.56−17.75
Wu et al.[173]	40	square	computational fluid dynamics	17.39−53.7
De Gans et al.[174]	30−100	square	polystyrene nanoparticle inks	21−91
Szczech et al.[175]	60	bipolar	nanoparticle suspension	23.1−47.9
Perelaer et al.[176]	70	square	polystyrene in toluene	23.5−66.8
Shin et al.[177]	50	square	ethylene glycol/ water mixture	35.5
Son et al.[178]	50	bipolar	water	58.8
Gan et al.[179]	50	square+ bipolar	water	60.4
Dong et al.[180]	53	single/ double	water	62.2

https://doi.org/10.1021/acsami.1c04544
ACS Appl. Mater. Interfaces XXXX, XXX, XXX−XXX

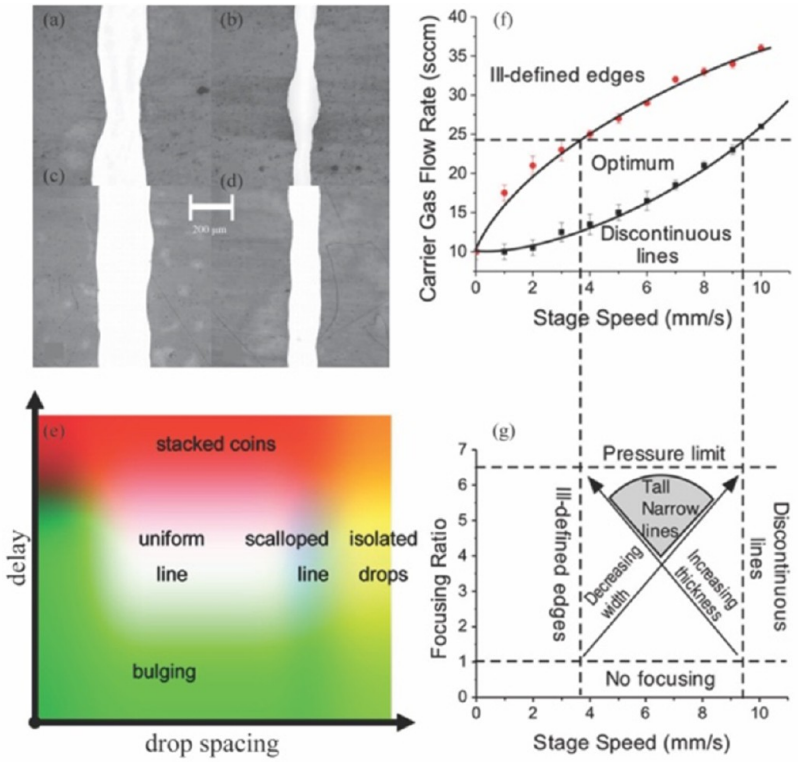

Figure 10. Printed line morphology optimization. (a–d) Influence of print speed and droplet distance on printed line morphology. Reprinted with permission from ref 184. Copyright 2009 Elsevier. (e) Developed empirical operating window for printed line morphology optimization of IJP. Reprinted with permission from ref 100. Copyright 2008 American Chemical Society. (f, g) Developed empirical operating window for printed line morphology optimization of AJP. Reprinted with permission from ref132. Copyright 2013 American Chemical Society.

Table 5. Examples of Droplet Control Based on Process Modeling of IJP

ref	ink	control parameters	control output
Chen et al.[185]	methanol/water, caffeine/water, protein/water	driving voltage, pulse width	droplet volume/mass
Wu et al.[186]	bioink	polymer concentration, excitation voltage, dwell time, rise time	droplet velocity, droplet volume
Wang et al.[187]	terpineol, methanol, CGO powder	pressure, nozzle opening time	droplet volume, droplet velocity
Gan et al.[179]	PEDOT ink	waveforms, amplitudes, pulse durations	droplet volume
Gao et al.[188]	Na-Alg solution	voltage amplitude, dwell time, frequency, concentration	droplet diameter, droplet velocity
Herran et al.[189]	sodium alginate solution	frequency, concentrations, dwell and echo times, voltage rise/fall times, excitation voltage amplitudes	droplet diameter

window with respect to gas flow rates was identified to print lines with better width ratio. Additionally, Mahajan et al.[132] investigated the effect of the interaction between the process speed and the gas ratio (SHGFR/CGFR) on the line morphology experimentally, and a process window as shown in Figure 10c, d was identified to print lines with a high aspect ratio and high resolution.

3.3. Printed Line Width Controllability. As process modeling plays a pivotal role in tailoring the printed line width of noncontact ink writing process, it is more receivable and has attracted great attention over the years. For IJP, as the controllability of the ejected droplet has a direct impact on the printed line width, various empirical models with respect to droplet size/volume/mass/velocity (Table 5) were developed to ensure the process controllability, which will be beneficial to customized line width printing. Different from IJP, the simplified analytical model[190] and empirical model[132] of AJP were developed to predict the printed line width directly, and the experiments validated the effectiveness of the proposed models.

However, as shown in Figure 11, because of the widening effect and thermal instability of the inks,[186,191−193] the proposed traditional modeling approaches were limited to determine the basic trend of the printed line morphology. To gain high controllability on the produced line width, it is crucial to fully understand the printing mechanisms and quantify the correlations between key control parameters and the printed line features accurately. Therefore, various computational fluid dynamics (CFD) models based on specific printing systems and model simplifications were developed for quantitative analysis of noncontact ink writing process. Salary et al.[127] developed a 2D-CFD model to elucidate the effect of the aerodynamic interaction between gas flow rates on the printed line width. Feng[194] proposed a simplified 3D-CFD model to investigate the impact of working height and nozzle taper angle on the printed droplet diameter. On the basis of a

https://doi.org/10.1021/acsami.1c04544
ACS Appl. Mater. Interfaces XXXX, XXX, XXX−XXX

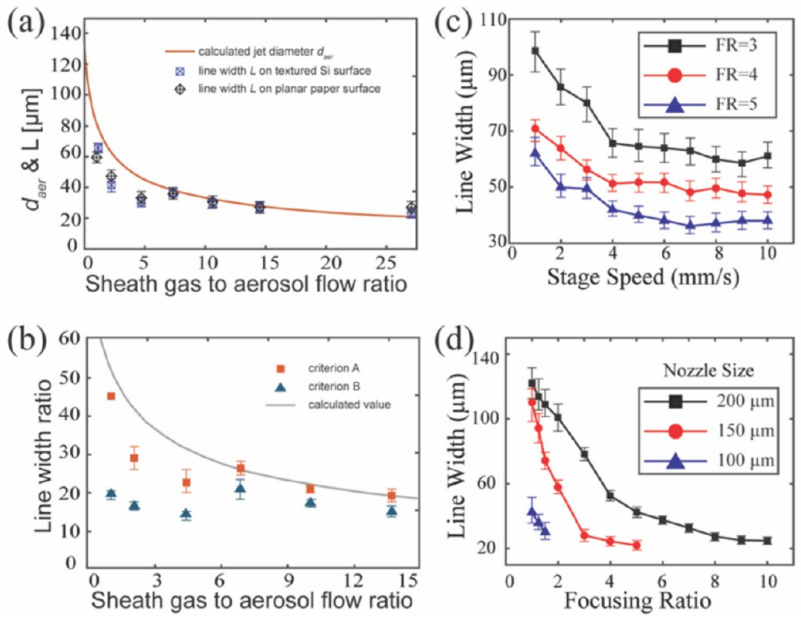

Figure 11. Printed line width modeling. (a, b) Simplified analytical model of AJP. Reprinted with permission from ref.190. Copyright 2014 Taylor & Francis. (c, d) Developed empirical model of AJP. Reprinted with permission from ref 132. Copyright 2013 American Chemical Society.

full 3D-CFD model of AJP, Chen et al.[195] pinpointed the influence of gas flow rates and particle size on the printed line morphology, and the line width was quantified on the basis of the provided the trajectories of the ink particles. However, as the CFD models have been developed based on specific printing systems and model simplifications, it can be impractical and computation heavy to develop a high-precision CFD model for general usability, which will hinder its applications in real-time printing process optimization.

3.4. Calibration of Process Drift. As the process drift can be attributed to changes of different sources, such as variations in ink viscosity, atomization efficiency, and deposition rate, various methods for system compensation have been proposed to improve print consistency qualitatively. Lall et al.[196] proposed a function of process capability ratio (index) to analyze the impact of control parameters on printing consistency, and a 10 h continuous print demonstrated that the ink viscosity and bubbler play an important role in maintaining print consistency. On the basis of numerical modeling and focused experiments, Secor[163] found that the interaction between annular drying caused by the sheath gas and impaction had a great impact on system drift, and a novel strategy that integrated a solvent bubbler with sheath gas was proposed to reduce process sensitivity and system drift. Similarly, as the ink temperature affected the stability of the atomization process directly, Lu et al.[106] introduced an ink bath temperature optimization approach to ensure the printing uniformity and printing stability, which was beneficial to printed device consistency and large-scale production. Besides ink temperature, as ink level variation also significantly induced atomization instability, an ink recirculation system was developed to maintain the ink level within the cartridge by Tafoya and Secor,[107] which provided a general strategy to overcome persistent issues of process instability and mitigate drift. Moreover, different in-process measuring systems with respect to deposition rate[108,164] and printed line morphology[197,198] were adopted to rectify the drift process in real time, which could serve as a potential method for real-time control of process drift and batch-to-batch variability.

4. MACHINE LEARNING APPROACHES FOR PROCESS OPTIMIZATION

Despite various traditional approaches being proposed as guidance for process optimization in noncontact writing techniques, because of the insufficient exploration of a design space and lack of a quantitative criterion to evaluate printing quality, they were limited to optimizing the basic trend of the printing process and improving the overall printing quality qualitatively. Different from traditional approaches, machine learning has the potential for efficient process optimization by introducing new process modeling and optimization methods, but the benefits of applying the machine learning to noncontact direct inking writing are recently being realized with research conducted into process optimization. In this section, the overview of machine learning techniques is provided in Section 4.1; following that, the state-of-the-art machine learning approaches for optimizing the noncontact ink writing process are reviewed in Sections 4.2 to 4.5.

4.1. Overview of Machine Learning Techniques. Machine learning is a branch of artificial intelligence, which is based on the concept that a system can identify hidden model patterns and make decisions with minimal human intervention. However, different from rule-based artificial intelligence, the machine learning can automatically train from data, and develop data-driven models with the ability of learning to perform specific tasks. Generally, machine learning approaches can be classified into three main types: (1) supervised learning, (2) unsupervised learning, and (3) reinforcement learning. The task of the supervised learning is to learn a function that maps an input to an output based on collected input−output pairs. Specifically, there are two main types of supervised learning algorithms: regression algorithms (such as artificial neural network, Bayesian regression, and support vector regression) and classification algorithms (such as decision tree, random forest and support vector machine).

https://doi.org/10.1021/acsami.1c04544
ACS Appl. Mater. Interfaces XXXX, XXX, XXX−XXX

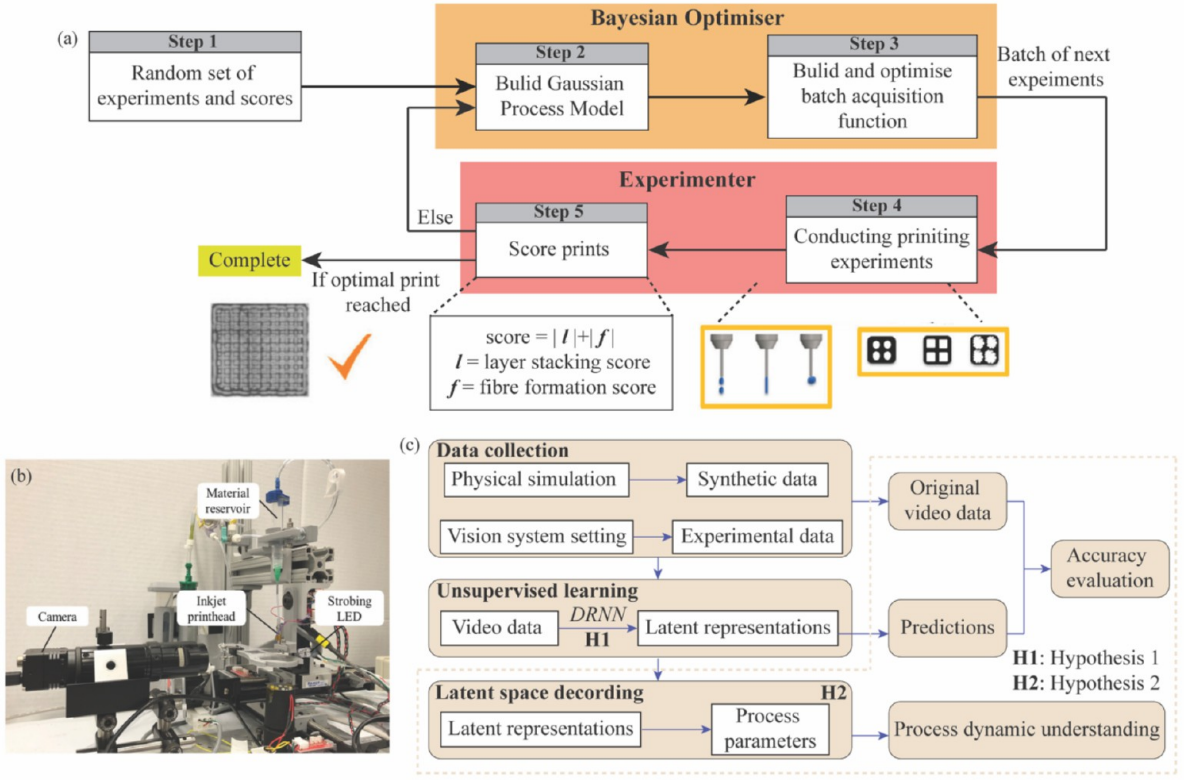

Figure 12. Ink printability identification of IJP. (a) Proposed Bayesian optimization framework for printability evaluation Reprinted with permission from ref 202. Copyright 2021 Elsevier. (b, c) Real-time data collection system and the designed framework for vision data learning of IJP. Reprinted with permission from ref 204. Copyright 2020 Elsevier.

The difference between these two types of supervised learning algorithms is that the former can map the input space into a real-value domain, whereas the latter can map the input space into predefined classes. Unlike supervised learning, unsupervised learning is a type of machine learning in which the models are trained using an unlabeled data set (i.e., without prescribed categories or priori grouping information in the data) and allowed to identify the hidden patterns from the given data set without any supervision. Unsupervised learning algorithms can be categorized into two types of problems: clustering and association. The main task of a clustering algorithm such as K-means clustering, K-nearest neighbors, and hierarchal clustering is to automatically divide an unlabeled data set into different groups based on feature similarity other than being driven by a specific purpose. On the other hand, an association algorithm such as principal component analysis and singular value decomposition is used for identifying the hidden correlations between different variables in a large data set. Unlike the above-mentioned machine learning approaches, the reinforcement learning is a feedback-based machine learning approach in which an agent interacts with the environment by executing actions and learns to improve performance based on the received results of actions. As the agent will be rewarded for good action and punished for bad action, it will adjust states according to the feedback of the previous action to get the maximum positive rewards in the process of reinforcement learning. Therefore, reinforcement learning is especially suitable for solving sequential decision-making problems, such as game-playing and robotics.

4.2. Ink Printability. As machine learning can develop a black-box model with less experimental data, it is often employed to establish the correlations between the rheological properties and printability of IJP. For example, Lee et al.[199] adopted the relative least general generalization algorithm and multiple regression to classify the ink printability with respect to ink composition. Menon et al.[200] integrated physical models with a hierarchical machine learning algorithm to predict the ink printability using sparse data sets. Besides regression and classification, Shi et al.[201] integrated a fully connected neural network model with a multiobjective optimization method to ensure the droplet was printed with less satellites, small size and high speed. Ruberu et al.[202] coupled a Bayesian optimization framework (Figure 12a) with adaptive sampling to develop a scoring system for printability evaluation, thus accelerating the printability optimization with minimal number of experiments. Moreover, due to the growing demand for a rapid method for printability evaluation, Uzun-Per et al.[203] proposed an automatic image analysis approach to investigate the correlations between printing conditions and ink printability. Besides image analysis, as shown in Figure 12b, c, Huang et al.[204] employed a real-time video collection system with a deep learning method to develop the relationship between the droplet patterns and ink printability automatically, which is more efficient than static image-based optimization approaches.

As AJP is capable of processing high viscosity ink, most research has focused on optimizing process parameters to improve the ink printability. Using response surface methodology (RSM) and analysis of variance (ANOVA), Wang et al.[96] investigated the relationship between process parameters and

https://doi.org/10.1021/acsami.1c04544
ACS Appl. Mater. Interfaces XXXX, XXX, XXX−XXX

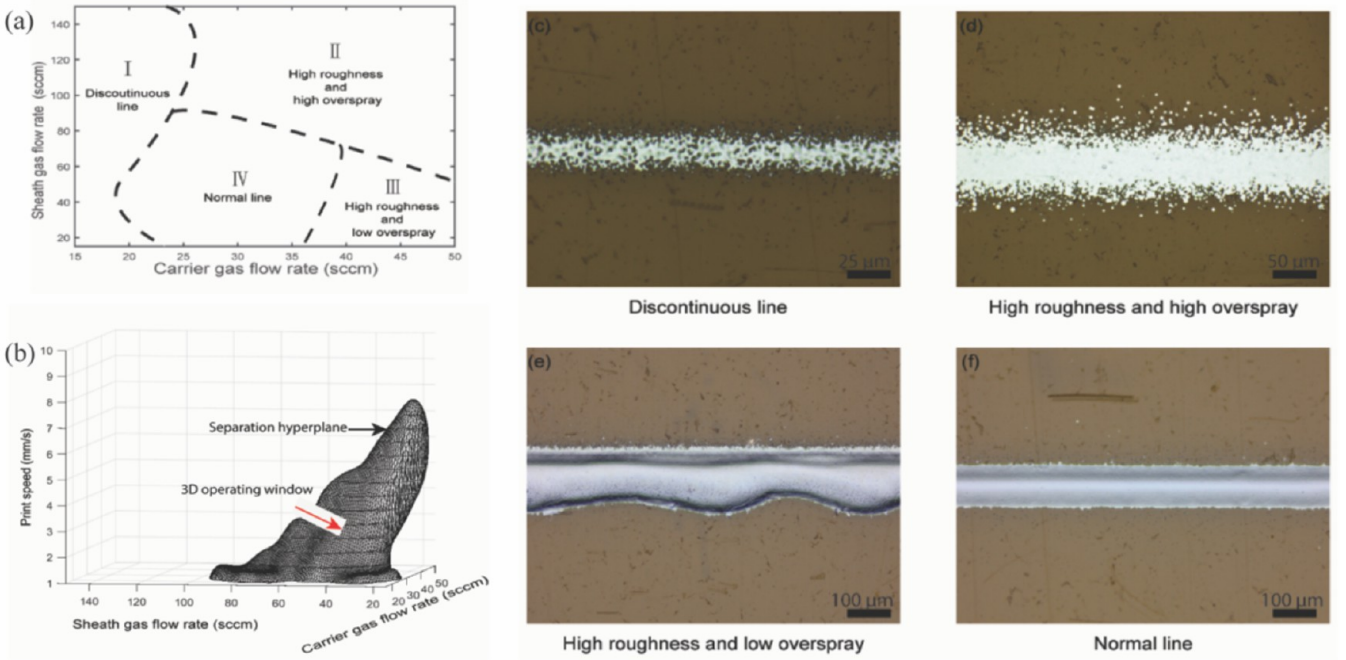

Figure 13. Printability analysis of AJP. Reprinted with permission from ref 205. Copyright 2019 American Chemical Society. (a) Printed line morphology was classified into four types based on K-means clustering in a 2D design space. (b) Identified 3D optimal operating window for printability optimization based on SVM. (c–f) Examples of different printed line morphology in a 2D design space.

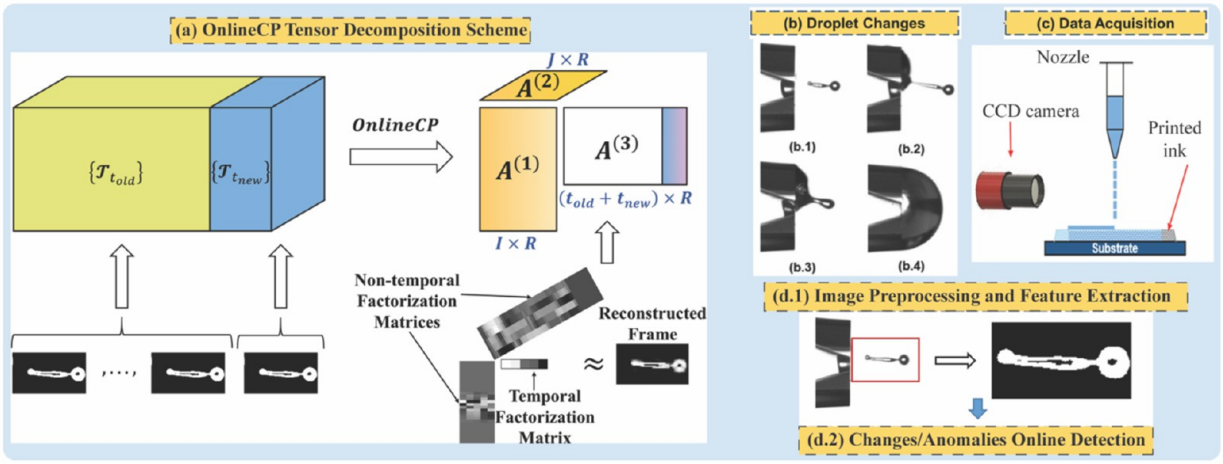

Figure 14. Proposed online droplet anomaly detection framework of IJP. Reprinted with permission from ref 208. Copyright 2021 Elsevier. (a) OnlineCP tensor decomposition approach. (b) Changes in the printed droplet. (c) Data acquisition system. (d) Online droplet anomaly detection process.

ink printability, and a criterion was proposed to reduce printed the line edge roughness and overspray in a design space. Salary et al.[127] extracted the printed line features based on an image processing approach, and the printing quality was quantified and optimized by a group of criteria, including line density, overspray index, and line discontinuity. Moreover, various classical machine learning methods were adopted to improve the printability of AJP. For example, as shown in Figure 13, K-means clustering was employed to analyze the distribution of printed line morphology of AJP, and a support vector machine (SVM) was further adopted to identify the optimal operating window to ensure the ink printability in a design space.[205]

4.3. Printed Line Morphology Optimization. Despite traditional optimization methods being used to preserve the printed line quality in IJP, the methods have limited applications in offline fashion, and online optimization remains a critical challenge. Under such circumstances, as the droplet behaviors extensively define the final produced line morphology in IJP, machine vision systems have been employed to inspect the dynamic droplet dispensing behavior in real time, which is beneficial to the formed line morphology. For example, Lies et al.[206] developed an in situ inspection system for e-jet printing using a real-time image processing technology, but the proposed machine vision system was limited to detect whether a filament is printed or not. Moreover, a droplet location detection algorithm was coupled with an online monitoring system to ensure the process repeatability and reproducibility;[207] however, the undetected droplet shape may influence the produced line morphology. To extract more features for online monitoring while satisfying

https://doi.org/10.1021/acsami.1c04544
ACS Appl. Mater. Interfaces XXXX, XXX, XXX−XXX

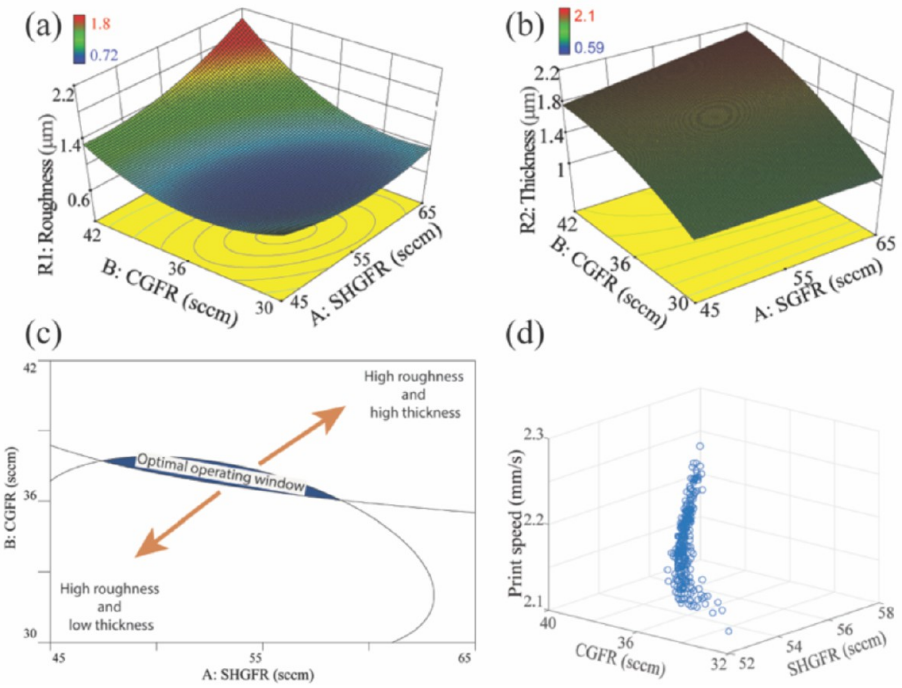

Figure 15. Printed line morphology optimization of AJP. Reprinted with permission from ref 151. Copyright 2020 Elsevier. (a, b) Derived line edge roughness model and line thickness model based on RSM. (c) Determined 2D optimal operating window based on a desirability function approach. (d) Obtained multiobjective optimization results in a 3D design space based on NSGA-III algorithm.

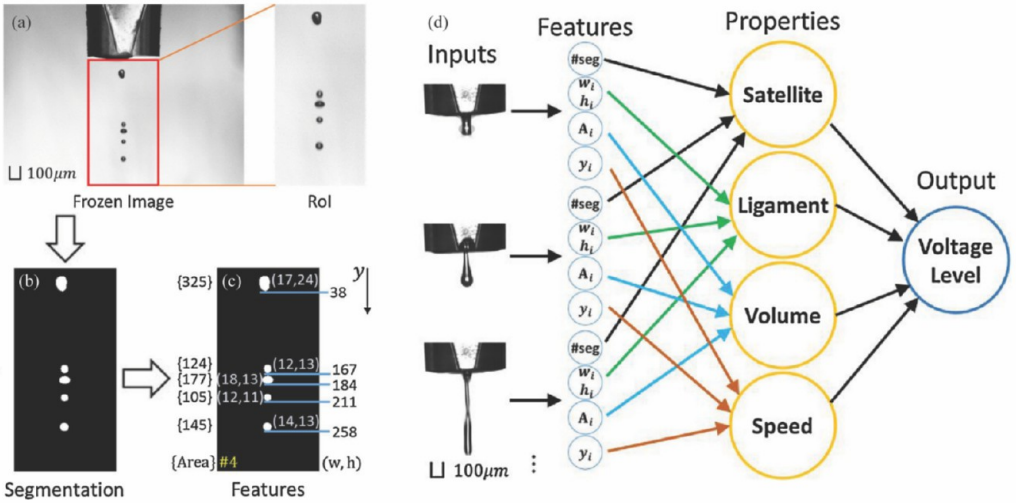

Figure 16. Machine learning-based droplet behaviors modeling. Reprinted with permission from ref 212. Copyright 2018 Elsevier. (a–c) Extract droplet behaviors from raw images. (d) Neural network modeling.

the requirement on detection efficiency, Segura et al.[208] adopted an online tensor decomposition approach to extract the features of droplet videos in real time, and a Bayesian online change detection framework was then employed to detect abnormal droplets from the online features. The proposed framework for online droplet anomaly detection is shown in Figure 14.

Different from IJP, as a conductive line is the basic component of AJP, previous research focused on directly optimizing the printed line morphology through process parameters. For example, as shown in Figure 15, Zhang et al.[151] investigated the conflicting relationship between line thickness and line edge roughness, then based on a desirability function approach and a nondominated sorting genetic algorithm III (NSGA-III). The inherent contradiction between printed line features was minimized in a 2D and 3D design space, respectively. However, the optimization efficiency was limited because of the adopted offline mode. On the contrary, based on online monitoring, Salary et al.[209] employed a shape-from-shading analysis method to recover the cross-sectional profile of printed electronic traces from the captured online images, which was helpful to improve the optimization efficiency of the printed line morphology and the homogeneity of device resistance. Moreover, as the objective of printed line morphology optimization was to achieve a high electrical performance of printed electronics, some studies investigated the relationship between offline images and the functional materials properties of printed electronics directly, which were

https://doi.org/10.1021/acsami.1c04544
ACS Appl. Mater. Interfaces XXXX, XXX, XXX−XXX

Table 6. Examples of Droplet Control Based on Process Modeling of IJP

ref	machine learning methods	model parameters	model output
Shi et al.[213]	multilayer perceptron network	print speed, voltage, nozzle diameter	droplet distance/ diameter
Wu et al.[133]	ensemble learning	polymer concentration, voltage, dwell time and rise time	droplet velocity/ volume
Ball et al.[214]	feed-forward neural network and genetic algorithm	standoff height, flow rate and voltage	droplet diameter
Tourloukis et al.[215]	nonlinear autoregressive neural network, Bayesian regularization, and scaled conjugate gradient algorithm	droplet volume, substrate temperature, drop velocity	geometry of the printed parts
Inyang-Udoh et al.[216]	back-propagation neural network and learning-based model	geometric proximity of nodes, ink flowability, and surface tension	droplet profile
He et al.[217]	decision tree, SVM, random forest, gradient boosting, and AdaBoosting	manufacturing velocity, PDMS thickness, duration of frame, and resin viscosity	print speed

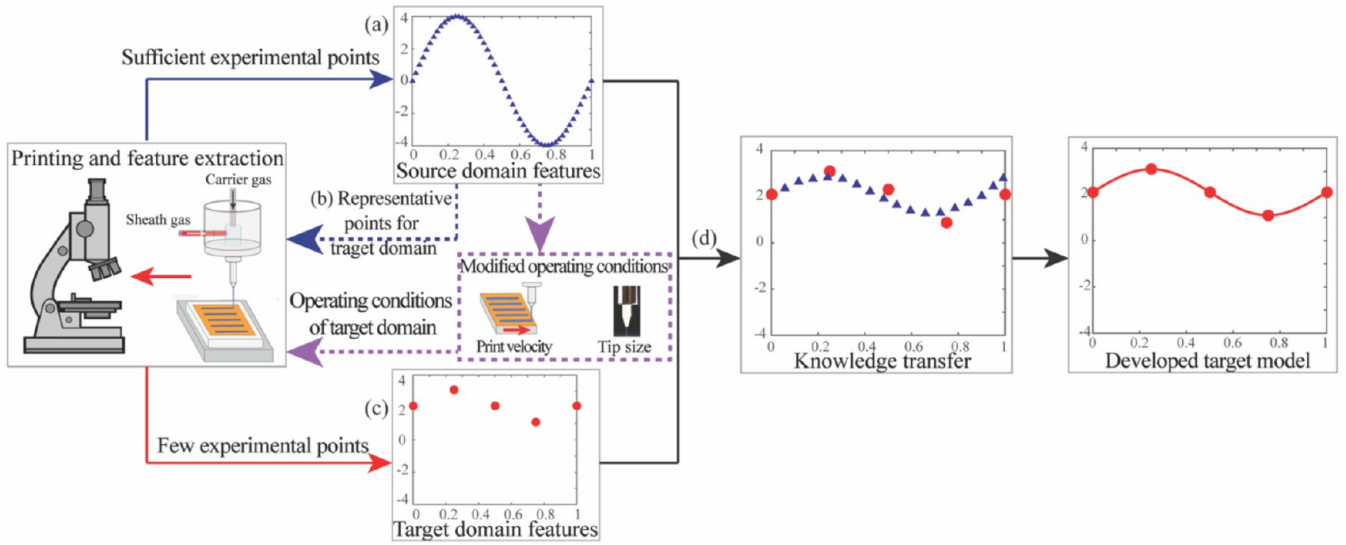

Figure 17. Illustration of the proposed knowledge transfer method for rapid process modeling and model migration. Reprinted with permission from ref 223. Copyright 2021 Elsevier. (a) Developing a sufficient source model. (b) Selection of the representative experimental points for target domain. (c) Data set collection in target domain. (d) Rapid process modeling and model migration based on knowledge transfer.

served as a potential method for online control of process drift. For example, based on a spatially correlated predictor, Li et al.[210] developed the correlations between the identified features from the raw images and printed line resistance. Yan et al.[211] introduced a SVM model to predict the printed sheet resistance with processed microscope images as inputs, and the prediction error (less than 10%) demonstrated the effectiveness of the proposed approach.

4.4. Printed Line Width Controllability. To preserve the controllability of the IJP process, several machine learning approaches were employed with vision based techniques for process modeling. For instance, as shown in Figure 16, Wang et al.[212] adopted an efficient image processing techniques to extract interpretable droplet behaviors from raw images, and a neural network model was adopted to develop the relationship between control parameters and droplet behaviors. Additionally, Table 6 describes various machine learning methods for droplet control in IJP. Despite the high controllability of droplet behaviors having a great impact on the printed line morphology, there is a need to further consider the droplet coalescence process and control the geometrical properties of printed lines directly.

To ensure high controllability of the printed line width, researchers adopted data-driven-based modeling methods to investigate the AJP process. For example, Chang[218] and Wang et al.[96] developed statistical models to investigate the influence of the main control parameters on the printed line features, and the effectiveness of the proposed models was validated by ANOVA and additional experiments. On the basis of the Gaussian process regression (GPR), Zhang et al.[219] investigated the inherent contradictions between line thickness, line edge roughness and a customized line width based on the integration of derived GPR models and NSGA-III. And the optimal process parameters for a specified line width were determined under the dual conflicting objectives of maximizing line thickness and minimizing line edge roughness, and the objective of customizing line width. The developed offline models were helpful to improve the controllability of the printed line width, but the modeling performance would be reduced due to the impact of random variations and process instability. Under such circumstances, the combination of a real-time process monitoring system and closed-loop control is an urgent need for a noncontact ink writing technology to further improve the process controllability. For instance, Lombardi et al.[197] proposed a PID closed-loop control system by integrating in situ process monitoring with a regression model on printed line features. The experimental results demonstrated the improved controllability of the printed line width, even in the presence of random variations and process drift.

4.5. Calibration of Process Drift. As traditional process drift compensation methods are limited to improve print

https://doi.org/10.1021/acsami.1c04544
ACS Appl. Mater. Interfaces XXXX, XXX, XXX−XXX

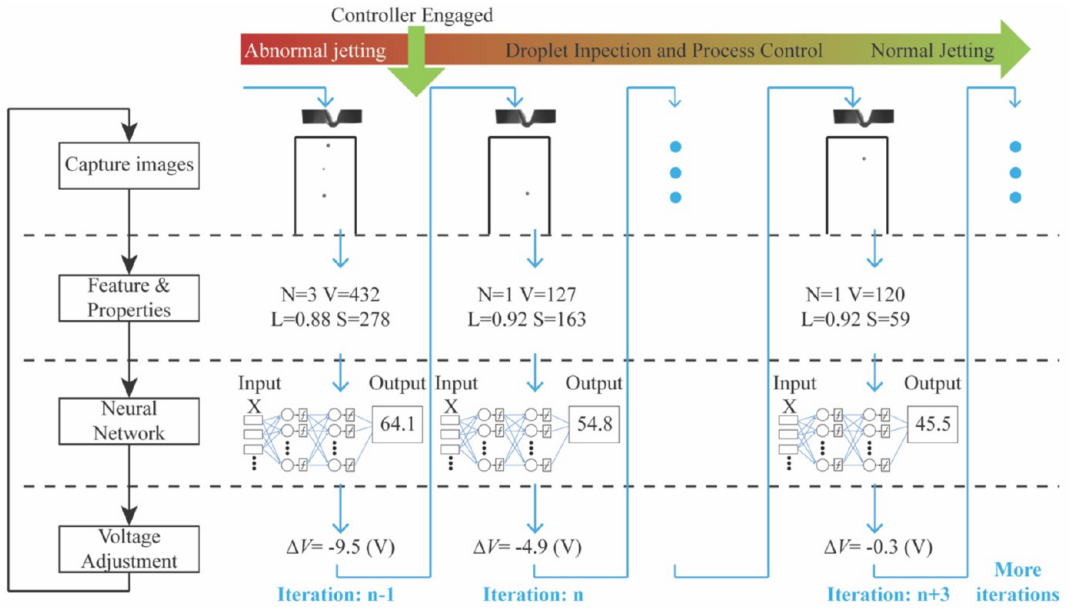

Figure 18. Case study to rectify the process drift through a closed-loop control system. Reprinted with permission from ref 212. Copyright 2018 Elsevier.

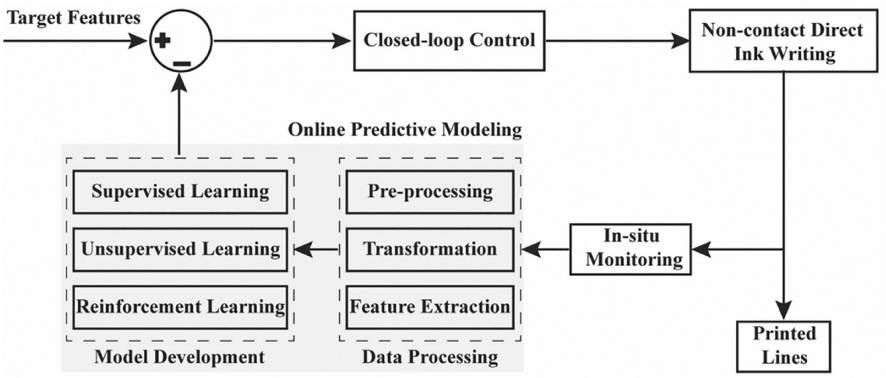

Figure 19. Illustration of a real-time monitoring and control system for online process optimization in the noncontact direct ink writing process.

consistency qualitatively, various machine learning based strategies have been proposed for process modeling on printed line features or electrical properties, which will contribute to the quantification and further compensation of process drift.

Because of the similar material processing and deposition mechanisms between varied working conditions,[220−222] a knowledge transfer-based method was proposed for rapid model migration of printed line features under different working conditions, as shown in Figure 17.[223] Despite the process drift being calibrated efficiently based on model migration, the compensation efficiency was restricted by the employed offline mode.

In this case, online monitoring of the printed line features was preferred to different studies for detecting the process drift in real time. For example, on the basis of the extracted printed line width[127] and cross-sectional profile[198] from online images, the process drift can be detected in a timely manner during the printing process. Moreover, the integration of an in situ monitoring system with closed-loop control was further employed in many research studies to improve the calibration efficiency. For instance, an online closed-loop control system for customized line width printing was helpful to correct the process drift in real time.[197] Wang et al.[212] proposed a closed-loop control framework by integrating a machine vision system with neural network-based process modeling on droplet behaviors. As shown in Figure 18, the proposed framework can automatically rectify the abnormal printed droplet features caused by process drift through tuning the input drive voltage.

In addition to geometrical properties, the online modeling of electrical properties was also employed to process drift calibration. On the basis of an optical measurement system, Tafoya et al.[224] proposed an online process modeling approach to correlate the process parameters with the electrical resistance of the printed patterns directly. Additionally, on the basis of a sparse representation intelligent classification model, Salary et al.[225] classified the printed line resistance as a function of main process parameters and the extracted printed line features. Therefore, the process drift can be rectified in real time based on the predicted electrical properties and the adopted closed-loop control system.

5. CONCLUSIONS

In this paper, we provided an overview of the noncontact direct ink writing technologies with advantages and disadvantages and reviewed current research progress on process optimization with respect to IJP and AJP techniques. Despite

https://doi.org/10.1021/acsami.1c04544
ACS Appl. Mater. Interfaces XXXX, XXX, XXX−XXX

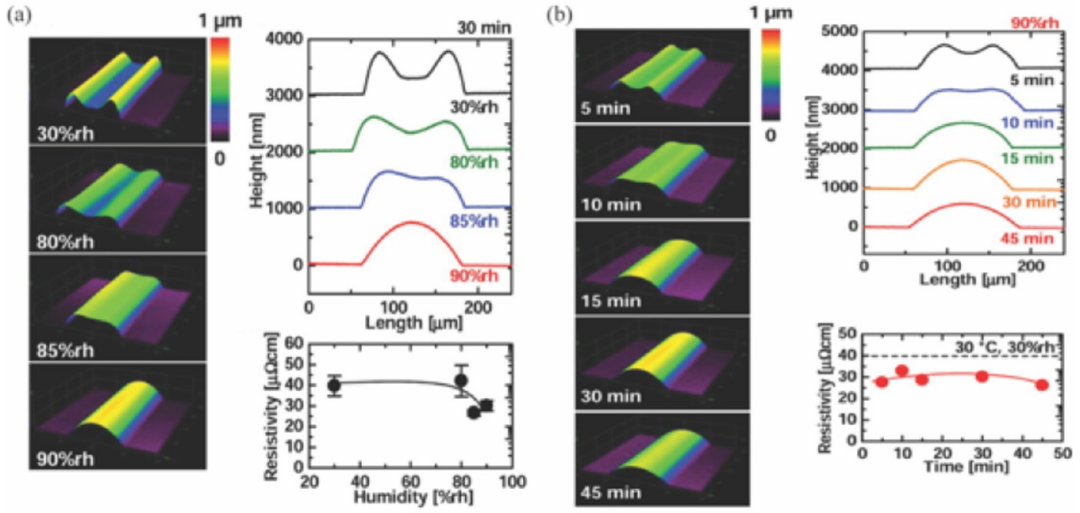

Figure 20. Influence of postprinting factors on printed line uniformity and electrical performance. Reprinted with permission from ref.233. Copyright 2013 American Chemical Society. (a) Controlling the profile and electrical performance of printed sliver lines by varying humidity with fixed temperature and drying time. (b) Controlling the profile and electrical performance of printed sliver lines by varying the drying time with fixed humidity and temperature.

various traditional approaches being proposed as guidance for process optimization in the noncontact direct ink writing techniques, they were limited to optimize the basic trend of printing process and improve the overall printing quality qualitatively, because of the insufficient exploration of a design space and lack of a quantitative criterion to evaluate printing quality. Compared with traditional approaches, machine learning had great potential for efficient process optimization, because of its novel process modeling and optimization methods. However, as the adopted machine learning based strategies were aimed at optimizing a specific aspect of the printing process, the benefits of applying the machine learning to noncontact direct inking writing were reduced. Therefore, a systematic process optimization approach that integrates the advantages of the state-of-the-art machine learning techniques is in demand to fully optimize the noncontact direct ink writing process, including ink printability, line morphology optimization, printed line width controllability and process drift calibration.

However, because of the impact of many changing factors during printing, such as temperature fluctuations, solvent evaporation, and random variations, the developed stationary machine learning strategies for process optimization may not suffice for printing quality assurance. Therefore, it is necessary to further integrate the advantages of in situ monitoring[226−230] and closed-loop control[231,232] for in-process diagnosis and online optimization without manual intervention, which will be helpful to ensure process stability and optimization efficiency during printing. As shown in Figure 19, a systematic process optimization approach for noncontact direct ink writing consists of three main parts: (1) in situ monitoring, (2) online predictive modeling, and (3) closed-loop control. The corresponding optimization procedure consists of three phases. In the initial phase, the line samples will be printed based on the designed experimental points, and the printed line morphology can be captured using in situ monitoring. Then, based on real-time stream data processing, classical machine learning techniques such as clustering and classification can be utilized to analyze the distribution of printed line morphology and identify the optimal operating window systematically. In phase 2, based on the identified operating window and extracted line features such as line width, line thickness, and line edge roughness, the predictive regression models of geometrical properties can be developed and updated by using the state-of-the-art supervised learning techniques, such as artificial neural network, Bayesian regression and support vector regression. Then, the optimal parameters for customized line width can be identified based on multiobjective optimization to print the line with sufficient thickness and less edge roughness. If high controllability of the printed line features is required or the printing process is detected to have an uncontrollable drift trend, the developed predictive models will be integrated with a closed-loop control approach in phase 3, which will be helpful to ensure process controllability and stability during printing. Different from the machine learning-based strategies that are limited to optimizing a specific aspect of the printing process, the three phases of the proposed approach are aimed at improving the ink printability, optimizing the printed line morphology, and ensuring process controllability as well as stability. On the basis of the proposed optimization procedure, the main limitations of the noncontact direct ink writing process can be resolved in three phases. Therefore, compared with the exiting optimization strategies, the entire printing process has the potential to be fully optimized, which will be helpful to print lines with sufficient thickness, less edge roughness, and lower overspray while maintaining the customized line width.

Although the proposed approach has the potential to realize the systematic optimization of the noncontact direct ink writing process, the major requirements and challenges of introducing process monitoring and online optimization techniques into a noncontact direct ink writing technology are as follows: (1) in situ monitoring. As the basic elements of noncontact ink writing techniques are printed in micrometers, the capability of accurately capturing the printing features at high speed is crucial for an in situ monitoring system. Moreover, it will be challenging but important for the in situ monitoring system to recover multidimensional information from the simplified 2D information. (2) Online predictive modeling. Despite the state-of-the-art data-driven-based

https://doi.org/10.1021/acsami.1c04544
ACS Appl. Mater. Interfaces XXXX, XXX, XXX−XXX

regression approaches being more suitable for developing the predictive regression models of geometrical properties, the online identification of the key process parameters from various influencing factors will be a significant challenge because of the drifting nature of the printing processes. (3) Closed-loop control. Different from traditional model-based control approaches, the data-driven-based feedback control has new challenges in ensuring the robustness and stability of the printing processes. Moreover, the data-driven-based controller should have the capability of fast convergence, which will be helpful to reduce material waste during the control process.

Despite the real-time control and online process optimization of the printing quality being considered as the main challenge in previous research, the postprinting process will greatly affect the printed line uniformity because of the coffee-ring effect. For example, as shown in Figure 20, the ambient humidity and sintering time can influence the uniformity of the cross-sectional profile,[233] the conductive line will be printed inhomogeneously and prevented from being adopted to electronic devices that require excellent electrical performance. Therefore, it is important to develop a postprinting optimization approach to improve the uniformity of the cross-sectional profile. Moreover, because of the complex interaction between postprinting factors, a machine-learning-based approach is more suitable for postprinting process optimization because of its high modeling performance and low requirements of prior knowledge. In this case, based on machine learning, the online printing process optimization and offline postprinting process optimization can be integrated as a data-driven-based framework to systematically optimize the entire fabrication process of the noncontact ink writing technologies for printing electronics.

In this paper, we discussed the printing principles, key influencing factors, and main limitations of the noncontact direct ink writing technologies based on IJP and AJP. Then, traditional experimental methods and the state-of-the-art machine learning-based techniques adopted in IJP and AJP for process optimization were reviewed and discussed. Compared with traditional approaches, machine learning can achieve high modeling efficiency because of the low requirements of prior process knowledge. Moreover, as the machine learning can explore and identify the hidden knowledge of the material deposition process rather than relying on a lot of repetitive experiments, optimization efficiency can be significantly improved. However, as the adopted machine learning methods were aimed at optimizing a specific aspect of the printing process, the benefits of applying the machine learning to noncontact direct inking writing were reduced. Therefore, a systematic machine learning approach with the capabilities of real-time monitoring, online modeling, self-decision-making, and closed-loop control was proposed to improve the consistency and repeatability of printing process. The challenges and major limitations of the proposed approach were also highlighted in this paper. On the other hand, despite the proposed data-driven-based framework having the potential to realize the systematic optimization of the noncontact direct ink writing process, it is necessary to further integrate a numerical model to theoretically analyze and elucidate the ink transport and deposition mechanisms of the ink print system. Moreover, because of the influence of uncertain parameters, the printed line morphology will be produced with variations. Therefore, a stochastic model is needed to analyze the sensitivity for uncertain parameters and quantify the influence of the input uncertainties on the printing quality in future research work.

AUTHOR INFORMATION

Corresponding Author

Seung Ki Moon − *School of Mechanical and Aerospace Engineering, Nanyang Technological University, Singapore 639798, Singapore;* orcid.org/0000-0002-2249-7500; Email: skmoon@ntu.edu.sg

Author

Haining Zhang − *Faculty of Mechanical and Electrical Engineering, Kunming University of Science and Technology, Kunming 650500, China; School of Mechanical and Aerospace Engineering, Nanyang Technological University, Singapore 639798, Singapore;* orcid.org/0000-0003-2132-8091

Complete contact information is available at: https://pubs.acs.org/10.1021/acsami.1c04544

Notes

The authors declare no competing financial interest.

ACKNOWLEDGMENTS

This research work was partially supported by Korea Institute of Materials Science and Singapore Centre for 3D printing, Nanyang Technological University.

REFERENCES

(1) Espalin, D.; Muse, D. W.; MacDonald, E.; Wicker, R. B. 3D Printing Multifunctionality: Structures with Electronics. *Int. J. Adv. Manuf. Technol.* **2014**, *72* (5−8), 963−978.

(2) Wallin, T. J.; Pikul, J.; Shepherd, R. F. 3D Printing of Soft Robotic Systems. *Nat. Rev. Mater.* **2018**, *3* (6), 84−100.

(3) Bogue, R. 3D Printing: An Emerging Technology for Sensor Fabrication. *Sens. Rev.* **2016**, *36* (4), 333−338.

(4) Chang, J. S.; Facchetti, A. F.; Reuss, R. A Circuits and Systems Perspective of Organic/Printed Electronics: Review, Challenges, and Contemporary and Emerging Design Approaches. *IEEE J. Emerg. Sel. Top. Circuits Syst.* **2017**, *7* (1), 7−26.

(5) Park, S.; Vosguerichian, M.; Bao, Z. A Review of Fabrication and Applications of Carbon Nanotube Film-Based Flexible Electronics. *Nanoscale* **2013**, *5* (5), 1727−1752.

(6) Saengchairat, N.; Tran, T.; Chua, C.-K. A Review: Additive Manufacturing for Active Electronic Components. *Virtual Phys. Prototyp.* **2017**, *12* (1), 31−46.

(7) Valentine, A. D.; Busbee, T. A.; Boley, J. W.; Raney, J. R.; Chortos, A.; Kotikian, A.; Berrigan, J. D.; Durstock, M. F.; Lewis, J. A. Hybrid 3D Printing of Soft Electronics. *Adv. Mater.* **2017**, *29* (40), 1703817.

(8) Zeng, W.; Shu, L.; Li, Q.; Chen, S.; Wang, F.; Tao, X.-M. Fiber-Based Wearable Electronics: A Review of Materials, Fabrication, Devices, and Applications. *Adv. Mater.* **2014**, *26* (31), 5310−5336.

(9) Huang, L.; Huang, Y.; Liang, J.; Wan, X.; Chen, Y. Graphene-Based Conducting Inks for Direct Inkjet Printing of Flexible Conductive Patterns and Their Applications in Electric Circuits and Chemical Sensors. *Nano Res.* **2011**, *4* (7), 675−684.

(10) Kamyshny, A.; Magdassi, S. Conductive Nanomaterials for Printed Electronics. *Small* **2014**, *10* (17), 3515−3535.

(11) Berggren, M.; Nilsson, D.; Robinson, N. D. Organic Materials for Printed Electronics. *Nat. Mater.* **2007**, *6* (1), 3−5.

(12) Farahani, R. D.; Dubé, M.; Therriault, D. Three-Dimensional Printing of Multifunctional Nanocomposites: Manufacturing Techniques and Applications. *Adv. Mater.* **2016**, *28* (28), 5794−5821.

(13) Wu, W. Inorganic Nanomaterials for Printed Electronics: A Review. *Nanoscale* **2017**, *9* (22), 7342−7372.

(14) Sekine, C.; Tsubata, Y.; Yamada, T.; Kitano, M.; Doi, S. Recent Progress of High Performance Polymer OLED and OPV Materials for Organic Printed Electronics. *Sci. Technol. Adv. Mater.* **2014**, *15* (3), 034203.
(15) Fukuda, K.; Someya, T. Recent Progress in the Development of Printed Thin-Film Transistors and Circuits with High-Resolution Printing Technology. *Adv. Mater.* **2017**, *29* (25), 1602736.
(16) Cao, X.; Lau, C.; Liu, Y.; Wu, F.; Gui, H.; Liu, Q.; Ma, Y.; Wan, H.; Amer, Moh. R.; Zhou, C. Fully Screen-Printed, Large-Area, and Flexible Active-Matrix Electrochromic Displays Using Carbon Nanotube Thin-Film Transistors. *ACS Nano* **2016**, *10* (11), 9816−9822.
(17) Grau, G.; Subramanian, V. Fully High-Speed Gravure Printed, Low-Variability, High-Performance Organic Polymer Transistors with Sub-5 V Operation. *Adv. Electron. Mater.* **2016**, *2* (4), 1500328.
(18) Tong, S.; Sun, J.; Yang, J. Printed Thin-Film Transistors: Research from China. *ACS Appl. Mater. Interfaces* **2018**, *10* (31), 25902−25924.
(19) Gaikwad, A. M.; Steingart, D. A.; Nga Ng, T.; Schwartz, D. E.; Whiting, G. L. A Flexible High Potential Printed Battery for Powering Printed Electronics. *Appl. Phys. Lett.* **2013**, *102* (23), 233302.
(20) Giannakou, P.; Masteghin, M. G.; Slade, R. C. T.; Hinder, S. J.; Shkunov, M. Energy Storage on Demand: Ultra-High-Rate and High-Energy-Density Inkjet-Printed NiO Micro-Supercapacitors. *J. Mater. Chem. A* **2019**, *7* (37), 21496−21506.
(21) Cao, Z.; Koukharenko, E.; Tudor, M. J.; Torah, R. N.; Beeby, S. P. Flexible Screen Printed Thermoelectric Generator with Enhanced Processes and Materials. *Sens. Actuators, A* **2016**, *238*, 196−206.
(22) Grande, L.; Chundi, V. T.; Wei, D.; Bower, C.; Andrew, P.; Ryhänen, T. Graphene for Energy Harvesting/Storage Devices and Printed Electronics. *Particuology* **2012**, *10* (1), 1−8.
(23) Niu, S.; Matsuhisa, N.; Beker, L.; Li, J.; Wang, S.; Wang, J.; Jiang, Y.; Yan, X.; Yun, Y.; Burnett, W.; Poon, A. S. Y.; Tok, J. B.-H.; Chen, X.; Bao, Z. A Wireless Body Area Sensor Network Based on Stretchable Passive Tags. *Nat. Electron.* **2019**, *2* (8), 361−368.
(24) Rivadeneyra, A.; Fernández-Salmerón, J.; Agudo, M.; López-Villanueva, J. A.; Capitan-Vallvey, L. F.; Palma, A. J. Design and Characterization of a Low Thermal Drift Capacitive Humidity Sensor by Inkjet-Printing. *Sens. Actuators, B* **2014**, *195*, 123−131.
(25) Arapov, K.; Jaakkola, K.; Ermolov, V.; Bex, G.; Rubingh, E.; Haque, S.; Sandberg, H.; Abbel, R.; de With, G.; Friedrich, H. de; Friedrich, H. Graphene Screen-Printed Radio-Frequency Identification Devices on Flexible Substrates. *Phys. Status Solidi RRL* **2016**, *10* (11), 812−818.
(26) Subramanian, V.; Frechet, J. M. J.; Chang, P. C.; Huang, D. C.; Lee, J. B.; Molesa, S. E.; Murphy, A. R.; Redinger, D. R.; Volkman, S. K. Progress Toward Development of All-Printed RFID Tags: Materials, Processes, and Devices. *Proc. IEEE* **2005**, *93* (7), 1330−1338.
(27) Han, T.; Kundu, S.; Nag, A.; Xu, Y. 3D Printed Sensors for Biomedical Applications: A Review. *Sensors* **2019**, *19* (7), 1706.
(28) Vena, A.; Sydänheimo, L.; Tentzeris, M. M.; Ukkonen, L. A Fully Inkjet-Printed Wireless and Chipless Sensor for CO2 and Temperature Detection. *IEEE Sens. J.* **2015**, *15* (1), 89−99.
(29) Papazoglou, S.; Tsouti, V.; Chatzandroulis, S.; Zergioti, I. Direct Laser Printing of Graphene Oxide for Resistive Chemosensors. *Opt. Laser Technol.* **2016**, *82*, 163−169.
(30) Song, J.-H.; Kim, H.-J.; Kim, M.-S.; Min, S.-H.; Wang, Y.; Ahn, S.-H. Direct Printing of Performance Tunable Strain Sensor via Nanoparticle Laser Patterning Process. *Virtual Phys. Prototyp.* **2020**, *15* (3), 265−277.
(31) Carter, J. C.; Alvis, R. M.; Brown, S. B.; Langry, K. C.; Wilson, T. S.; McBride, M. T.; Myrick, M. L.; Cox, W. R.; Grove, M. E.; Colston, B. W. Fabricating Optical Fiber Imaging Sensors Using Inkjet Printing Technology: A PH Sensor Proof-of-Concept. *Biosens. Bioelectron.* **2006**, *21* (7), 1359−1364.
(32) Emon, M. O. F.; Alkadi, F.; Philip, D. G.; Kim, D.-H.; Lee, K.-C.; Choi, J.-W. Multi-Material 3D Printing of a Soft Pressure Sensor. *Addit. Manuf.* **2019**, *28*, 629−638.
(33) Mieloszyk, M.; Andrearczyk, A.; Majewska, K.; Jurek, M.; Ostachowicz, W. Polymeric Structure with Embedded Fiber Bragg Grating Sensor Manufactured Using Multi-Jet Printing Method. *Measurement* **2020**, *166*, 108229.
(34) Reddy, A. S. G.; Narakathu, B. B.; Atashbar, M. Z.; Rebros, M.; Rebrosova, E.; Bazuin, B. J.; Joyce, M. K.; Fleming, P. D.; Pekarovicova, A. Printed Capacitive Based Humidity Sensors on Flexible Substrates. *Sens. Lett.* **2011**, *9* (2), 869−871.
(35) Soni, M.; Bhattacharjee, M.; Ntagios, M.; Dahiya, R. Printed Temperature Sensor Based on PEDOT: PSS-Graphene Oxide Composite. *IEEE Sens. J.* **2020**, *20* (14), 7525−7531.
(36) Leigh, S. J.; Purssell, C. P.; Billson, D. R.; Hutchins, D. A. Using a Magnetite/Thermoplastic Composite in 3D Printing of Direct Replacements for Commercially Available Flow Sensors. *Smart Mater. Struct.* **2014**, *23* (9), 095039.
(37) Wilkinson, N. J.; Smith, M. a. A.; Kay, R. W.; Harris, R. A. A Review of Aerosol Jet Printing—a Non-Traditional Hybrid Process for Micro-Manufacturing. *Int. J. Adv. Manuf. Technol.* **2019**, *105* (11), 4599−4619.
(38) Torrisi, F.; Hasan, T.; Wu, W.; Sun, Z.; Lombardo, A.; Kulmala, T. S.; Hsieh, G.-W.; Jung, S.; Bonaccorso, F.; Paul, P. J.; Chu, D.; Ferrari, A. C. Inkjet-Printed Graphene Electronics. *ACS Nano* **2012**, *6* (4), 2992−3006.
(39) Kamyshny, A.; Steinke, J.; Magdassi, S. Metal-Based Inkjet Inks for Printed Electronics. *Open Appl. Phys. J.* **2011**, *4* (1), 19−36.
(40) Paulsen, J. A.; Renn, M.; Christenson, K.; Plourde, R. Printing Conformal Electronics on 3D Structures with Aerosol Jet Technology. *In 2012 Future of Instrumentation International Workshop (FIIW) Proceedings* **2012**, 1−4.
(41) He, P.; Cao, J.; Ding, H.; Liu, C.; Neilson, J.; Li, Z.; Kinloch, I. A.; Derby, B. Screen-Printing of a Highly Conductive Graphene Ink for Flexible Printed Electronics. *ACS Appl. Mater. Interfaces* **2019**, *11* (35), 32225−32234.
(42) Ostfeld, A. E.; Deckman, I.; Gaikwad, A. M.; Lochner, C. M.; Arias, A. C. Screen Printed Passive Components for Flexible Power Electronics. *Sci. Rep.* **2015**, *5* (1), 1−11.
(43) Hyun, W. J.; Secor, E. B.; Hersam, M. C.; Frisbie, C. D.; Francis, L. F. High-Resolution Patterning of Graphene by Screen Printing with a Silicon Stencil for Highly Flexible Printed Electronics. *Adv. Mater.* **2015**, *27* (1), 109−115.
(44) Cen, J.; Kitsomboonloha, R.; Subramanian, V. Cell Filling in Gravure Printing for Printed Electronics. *Langmuir* **2014**, *30* (45), 13716−13726.
(45) Secor, E. B.; Lim, S.; Zhang, H.; Frisbie, C. D.; Francis, L. F.; Hersam, M. C. Gravure Printing of Graphene for Large-Area Flexible Electronics. *Adv. Mater.* **2014**, *26* (26), 4533−4538.
(46) Grau, G.; Cen, J.; Kang, H.; Kitsomboonloha, R.; Scheideler, W. J.; Subramanian, V. Gravure-Printed Electronics: Recent Progress in Tooling Development, Understanding of Printing Physics, and Realization of Printed Devices. *Flex. Print. Electron.* **2016**, *1* (2), 023002.
(47) Cho, C.-K.; Hwang, W.-J.; Eun, K.; Choa, S.-H.; Na, S.-I.; Kim, H.-K. Mechanical Flexibility of Transparent PEDOT:PSS Electrodes Prepared by Gravure Printing for Flexible Organic Solar Cells. *Sol. Energy Mater. Sol. Cells* **2011**, *95* (12), 3269−3275.
(48) Tang, N.; Zhou, C.; Xu, L.; Jiang, Y.; Qu, H.; Duan, X. A Fully Integrated Wireless Flexible Ammonia Sensor Fabricated by Soft Nano-Lithography. *ACS Sens.* **2019**, *4* (3), 726−732.
(49) Zhang, F.; Nyberg, T.; Inganäs, O. Conducting Polymer Nanowires and Nanodots Made with Soft Lithography. *Nano Lett.* **2002**, *2* (12), 1373−1377.
(50) Wisser, F. M.; Schumm, B.; Mondin, G.; Grothe, J.; Kaskel, S. Precursor Strategies for Metallic Nano- and Micropatterns Using Soft Lithography. *J. Mater. Chem. C* **2015**, *3* (12), 2717−2731.
(51) Kim, M.; Alrowais, H.; Pavlidis, S.; Brand, O. Size-Scalable and High-Density Liquid-Metal-Based Soft Electronic Passive Components and Circuits Using Soft Lithography. *Adv. Funct. Mater.* **2017**, *27* (3), 1604466.

https://doi.org/10.1021/acsami.1c04544
ACS Appl. Mater. Interfaces XXXX, XXX, XXX−XXX

(52) Serban, D. A.; Greco, P.; Melinte, S.; Vlad, A.; Dutu, C. A.; Zacchini, S.; Iapalucci, M. C.; Biscarini, F.; Cavallini, M. Towards All-Organic Field-Effect Transistors by Additive Soft Lithography. *Small* **2009**, *5* (10), 1117−1122.
(53) Choi, Y.-M.; Kim, K.-Y.; Lee, E.; Jo, J.; Lee, T.-M. Fabrication of a Single-Layer Metal-Mesh Touchscreen Sensor Using Reverse-Offset Printing. *J. Inf. Disp.* **2015**, *16* (1), 37−41.
(54) Choi, Y.-M.; Lee, E.; Lee, T.-M. Mechanism of Reverse-Offset Printing. *J. Micromech. Microeng.* **2015**, *25* (7), 075019.
(55) Choi, Y.-M.; Lee, E.-S.; Lee, T.-M.; Kim, K.-Y. Optimization of a Reverse-Offset Printing Process and Its Application to a Metal Mesh Touch Screen Sensor. *Microelectron. Eng.* **2015**, *134*, 1−6.
(56) Fukuda, K.; Yoshimura, Y.; Okamoto, T.; Takeda, Y.; Kumaki, D.; Katayama, Y.; Tokito, S. Reverse-Offset Printing Optimized for Scalable Organic Thin-Film Transistors with Submicrometer Channel Lengths. *Adv. Electron. Mater.* **2015**, *1* (8), 1500145.
(57) Kerndl, M.; Šteffan, P. Usage of Offset Printing Technology for Printed Electronics and Smart Labels. *In 2020 43rd International Conference on Telecommunications and Signal Processing (TSP)* **2020**, 637−639.
(58) Mariappan, D. D.; Kim, S.; Boutilier, M. S. H.; Zhao, J.; Zhao, H.; Beroz, J.; Muecke, U.; Sojoudi, H.; Gleason, K.; Brun, P.-T.; Hart, A. J. Dynamics of Liquid Transfer from Nanoporous Stamps in High-Resolution Flexographic Printing. *Langmuir* **2019**, *35* (24), 7659−7671.
(59) Maddipatla, D.; Narakathu, B. B.; Avuthu, S. G. R.; Emamian, S.; Eshkeiti, A.; Chlaihawi, A. A.; Bazuin, B. J.; Joyce, M. K.; Barrett, C. W.; Atashbar, M. Z. A Novel Flexographic Printed Strain Gauge on Paper Platform. *In 2015 IEEE SENSORS* **2015**, 1−4.
(60) Deganello, D.; Cherry, J. A.; Gethin, D. T.; Claypole, T. C. Patterning of Micro-Scale Conductive Networks Using Reel-to-Reel Flexographic Printing. *Thin Solid Films* **2010**, *518* (21), 6113−6116.
(61) Krebs, F. C.; Fyenbo, J.; Jørgensen, M. Product Integration of Compact Roll-to-Roll Processed Polymer Solar Cell Modules: Methods and Manufacture Using Flexographic Printing, Slot-Die Coating and Rotary Screen Printing. *J. Mater. Chem.* **2010**, *20* (41), 8994−9001.
(62) Cardoso, R. M.; Mendonça, D. M. H.; Silva, W. P.; Silva, M. N. T.; Nossol, E.; da Silva, R. A. B.; Richter, E. M.; Muñoz, R. A. A. 3D Printing for Electroanalysis: From Multiuse Electrochemical Cells to Sensors. *Anal. Chim. Acta* **2018**, *1033*, 49−57.
(63) Kim, K.; Park, J.; Suh, J.; Kim, M.; Jeong, Y.; Park, I. 3D Printing of Multiaxial Force Sensors Using Carbon Nanotube (CNT)/Thermoplastic Polyurethane (TPU) Filaments. *Sens. Actuators, A* **2017**, *263*, 493−500.
(64) Mousavi, S.; Howard, D.; Zhang, F.; Leng, J.; Wang, C. H. Direct 3D Printing of Highly Anisotropic, Flexible, Constriction-Resistive Sensors for Multidirectional Proprioception in Soft Robots. *ACS Appl. Mater. Interfaces* **2020**, *12* (13), 15631−15643.
(65) Ha, M.; Seo, J.-W. T.; Prabhumirashi, P. L.; Zhang, W.; Geier, M. L.; Renn, M. J.; Kim, C. H.; Hersam, M. C.; Frisbie, C. D. Aerosol Jet Printed, Low Voltage, Electrolyte Gated Carbon Nanotube Ring Oscillators with Sub-5 Ms Stage Delays. *Nano Lett.* **2013**, *13* (3), 954−960.
(66) Ha, M.; Xia, Y.; Green, A. A.; Zhang, W.; Renn, M. J.; Kim, C. H.; Hersam, M. C.; Frisbie, C. D. Printed, Sub-3V Digital Circuits on Plastic from Aqueous Carbon Nanotube Inks. *ACS Nano* **2010**, *4* (8), 4388−4395.
(67) Gupta, A. A.; Bolduc, A.; Cloutier, S. G.; Izquierdo, R. Aerosol Jet Printing for Printed Electronics Rapid Prototyping. *In 2016 IEEE International Symposium on Circuits and Systems (ISCAS)* **2016**, 866−869.
(68) Smith, M.; Choi, Y. S.; Boughey, C.; Kar-Narayan, S. Controlling and Assessing the Quality of Aerosol Jet Printed Features for Large Area and Flexible Electronics. *Flex. Print. Electron.* **2017**, *2* (1), 015004.
(69) Mashayekhi, M.; Winchester, L.; Evans, L.; Pease, T.; Laurila, M.; Mäntysalo, M.; Ogier, S.; Terés, L.; Carrabina, J. Evaluation of Aerosol, Superfine Inkjet, and Photolithography Printing Techniques for Metallization of Application Specific Printed Electronic Circuits. *IEEE Trans. Electron Devices* **2016**, *63* (3), 1246−1253.
(70) Agarwala, S.; Goh, G. L.; Dinh Le, T.-S.; An, J.; Peh, Z. K.; Yeong, W. Y.; Kim, Y.-J. Wearable Bandage-Based Strain Sensor for Home Healthcare: Combining 3D Aerosol Jet Printing and Laser Sintering. *ACS Sens.* **2019**, *4* (1), 218−226.
(71) Al-Milaji, K. N.; Huang, Q.; Li, Z.; Ng, T. N.; Zhao, H. Direct Embedment and Alignment of Silver Nanowires by Inkjet Printing for Stretchable Conductors. *ACS Appl. Electron. Mater.* **2020**, *2* (10), 3289−3298.
(72) Mannerbro, R.; Ranlöf, M.; Robinson, N.; Forchheimer, R. Inkjet Printed Electrochemical Organic Electronics. *Synth. Met.* **2008**, *158* (13), 556−560.
(73) Kim, H. S.; Kang, J. S.; Park, J. S.; Hahn, H. T.; Jung, H. C.; Joung, J. W. Inkjet Printed Electronics for Multifunctional Composite Structure. *Compos. Sci. Technol.* **2009**, *69* (7), 1256−1264.
(74) Secor, E. B.; Prabhumirashi, P. L.; Puntambekar, K.; Geier, M. L.; Hersam, M. C. Inkjet Printing of High Conductivity, Flexible Graphene Patterns. *J. Phys. Chem. Lett.* **2013**, *4* (8), 1347−1351.
(75) Yun, C.; Choi, J.; Kang, H. W.; Kim, M.; Moon, H.; Sung, H. J.; Yoo, S. Digital-Mode Organic Vapor-Jet Printing (D-OVJP): Advanced Jet-on-Demand Control of Organic Thin-Film Deposition. *Adv. Mater.* **2012**, *24* (21), 2857−2862.
(76) Arnold, M. S.; McGraw, G. J.; Forrest, S. R.; Lunt, R. R. Direct Vapor Jet Printing of Three Color Segment Organic Light Emitting Devices for White Light Illumination. *Appl. Phys. Lett.* **2008**, *92* (5), 053301.
(77) Shtein, M.; Peumans, P.; Benziger, J. B.; Forrest, S. R. Direct, Mask- and Solvent-Free Printing of Molecular Organic Semiconductors. *Adv. Mater.* **2004**, *16* (18), 1615−1620.
(78) Yun, C.; Moon, H.; Kang, H. W.; Kim, M.; Sung, H. J.; Yoo, S. High-Performance Pentacene Thin-Film Transistors Fabricated by Organic Vapor-Jet Printing. *IEEE Electron Device Lett.* **2010**, *31* (11), 1305−1307.
(79) Zhang, T.; Hu, M.; Liu, Y.; Guo, Q.; Wang, X.; Zhang, W.; Lau, W.; Yang, J. A Laser Printing Based Approach for Printed Electronics. *Appl. Phys. Lett.* **2016**, *108* (10), 103501.
(80) Luo, S.; Hoang, P. T.; Liu, T. Direct Laser Writing for Creating Porous Graphitic Structures and Their Use for Flexible and Highly Sensitive Sensor and Sensor Arrays. *Carbon* **2016**, *96*, 522−531.
(81) Ahmadraji, T.; Gonzalez-Macia, L.; Ritvonen, T.; Willert, A.; Ylimaula, S.; Donaghy, D.; Tuurala, S.; Suhonen, M.; Smart, D.; Morrin, A.; Efremov, V.; Baumann, R. R.; Raja, M.; Kemppainen, A.; Killard, A. J. Biomedical Diagnostics Enabled by Integrated Organic and Printed Electronics. *Anal. Chem.* **2017**, *89* (14), 7447−7454.
(82) Joe Lopes, A.; MacDonald, E.; Wicker, R. B. Integrating Stereolithography and Direct Print Technologies for 3D Structural Electronics Fabrication. *Rapid Prototyp. J.* **2012**, *18* (2), 129−143.
(83) Khan, Y.; Thielens, A.; Muin, S.; Ting, J.; Baumbauer, C.; Arias, A. C. A New Frontier of Printed Electronics: Flexible Hybrid Electronics. *Adv. Mater.* **2020**, *32* (15), 1905279.
(84) Sung, J.; Kang, B. J.; Oh, J. H. Fabrication of High-Resolution Conductive Lines by Combining Inkjet Printing with Soft Lithography. *Microelectron. Eng.* **2013**, *110*, 219−223.
(85) Kempa, H.; Hambsch, M.; Reuter, K.; Stanel, M.; Schmidt, G. C.; Meier, B.; Hubler, A. C. Complementary Ring Oscillator Exclusively Prepared by Means of Gravure and Flexographic Printing. *IEEE Trans. Electron Devices* **2011**, *58* (8), 2765−2769.
(86) Khan, S.; Lorenzelli, L.; Dahiya, R. S. Technologies for Printing Sensors and Electronics Over Large Flexible Substrates: A Review. *IEEE Sens. J.* **2015**, *15* (6), 3164−3185.
(87) Li, Q.; Zhang, J.; Li, Q.; Li, G.; Tian, X.; Luo, Z.; Qiao, F.; Wu, X.; Zhang, J. Review of Printed Electrodes for Flexible Devices. *Front. Mater.* **2019**, *5*, 77.
(88) Wu, W. Inorganic Nanomaterials for Printed Electronics: A Review. *Nanoscale* **2017**, *9* (22), 7342−7372.
(89) Moutinho, I. M. T.; Ferreira, P. J. T.; Figueiredo, M. L. Impact of Surface Sizing on Inkjet Printing Quality. *Ind. Eng. Chem. Res.* **2007**, *46* (19), 6183−6188.

https://doi.org/10.1021/acsami.1c04544
ACS Appl. Mater. Interfaces XXXX, XXX, XXX−XXX

(90) Kim, C.; Nogi, M.; Suganuma, K.; Yamato, Y. Inkjet-Printed Lines with Well-Defined Morphologies and Low Electrical Resistance on Repellent Pore-Structured Polyimide Films. *ACS Appl. Mater. Interfaces* **2012**, *4* (4), 2168−2173.
(91) Mahajan, A.; Frisbie, C. D.; Francis, L. F. Optimization of Aerosol Jet Printing for High-Resolution, High-Aspect Ratio Silver Lines. *ACS Appl. Mater. Interfaces* **2013**, *5* (11), 4856−4864.
(92) Kim, S. H.; Hong, K.; Lee, K. H.; Frisbie, C. D. Performance and Stability of Aerosol-Jet-Printed Electrolyte-Gated Transistors Based on Poly(3-Hexylthiophene). *ACS Appl. Mater. Interfaces* **2013**, *5* (14), 6580−6585.
(93) Yang, Q.; Li, H.; Li, M.; Li, Y.; Chen, S.; Bao, B.; Song, Y. Rayleigh Instability-Assisted Satellite Droplets Elimination in Inkjet Printing. *ACS Appl. Mater. Interfaces* **2017**, *9* (47), 41521−41528.
(94) Rosker, E. S.; Barako, M. T.; Nguyen, E.; DiMarzio, D.; Kisslinger, K.; Duan, D.-W.; Sandhu, R.; Goorsky, M. S.; Tice, J. Approaching the Practical Conductivity Limits of Aerosol Jet Printed Silver. *ACS Appl. Mater. Interfaces* **2020**, *12* (26), 29684−29691.
(95) Alhendi, M.; Sivasubramony, R. S.; Weerawarne, D. L.; Iannotti, J.; Borgesen, P.; Poliks, M. D. Assessing Current-Carrying Capacity of Aerosol Jet Printed Conductors. *Adv. Eng. Mater.* **2020**, *22* (11), 2000520.
(96) Wang, K.; Chang, Y.-H.; Zhang, C.; Wang, B. Evaluation of Quality of Printed Strain Sensors for Composite Structural Health Monitoring Applications. In *2013 Society for the Advancement of Material and Process Engineering (SAMPE) Fall Technical Conference*, 2013; pp 21−24.
(97) Lu, S.; Zheng, J.; Cardenas, J. A.; Williams, N. X.; Lin, Y.-C.; Franklin, A. D. Uniform and Stable Aerosol Jet Printing of Carbon Nanotube Thin-Film Transistors by Ink Temperature Control. *ACS Appl. Mater. Interfaces* **2020**, *12* (38), 43083−43089.
(98) Choi, S.; Stassi, S.; Pisano, A. P.; Zohdi, T. I. Coffee-Ring Effect-Based Three Dimensional Patterning of Micro/Nanoparticle Assembly with a Single Droplet. *Langmuir* **2010**, *26* (14), 11690−11698.
(99) Xu, J.; Du, J.; Jing, C.; Zhang, Y.; Cui, J. Facile Detection of Polycyclic Aromatic Hydrocarbons by a Surface-Enhanced Raman Scattering Sensor Based on the Au Coffee Ring Effect. *ACS Appl. Mater. Interfaces* **2014**, *6* (9), 6891−6897.
(100) Soltman, D.; Subramanian, V. Inkjet-Printed Line Morphologies and Temperature Control of the Coffee Ring Effect. *Langmuir* **2008**, *24* (5), 2224−2231.
(101) Sun, J.; Bao, B.; He, M.; Zhou, H.; Song, Y. Recent Advances in Controlling the Depositing Morphologies of Inkjet Droplets. *ACS Appl. Mater. Interfaces* **2015**, *7* (51), 28086−28099.
(102) Goh, G. L.; Agarwala, S.; Yeong, W. Y. Aerosol-Jet-Printed Preferentially Aligned Carbon Nanotube Twin-Lines for Printed Electronics. *ACS Appl. Mater. Interfaces* **2019**, *11* (46), 43719−43730.
(103) Sun, J.; Li, Y.; Liu, G.; Chen, S.; Zhang, Y.; Chen, C.; Chu, F.; Song, Y. Fabricating High-Resolution Metal Pattern with Inkjet Printed Water-Soluble Sacrificial Layer. *ACS Appl. Mater. Interfaces* **2020**, *12* (19), 22108−22114.
(104) Hondred, J. A.; Stromberg, L. R.; Mosher, C. L.; Claussen, J. C. High-Resolution Graphene Films for Electrochemical Sensing via Inkjet Maskless Lithography. *ACS Nano* **2017**, *11* (10), 9836−9845.
(105) Zhang, Q.; Shao, S.; Chen, Z.; Pecunia, V.; Xia, K.; Zhao, J.; Cui, Z. High-Resolution Inkjet-Printed Oxide Thin-Film Transistors with a Self-Aligned Fine Channel Bank Structure. *ACS Appl. Mater. Interfaces* **2018**, *10* (18), 15847−15854.
(106) Lu, S.; Zheng, J.; Cardenas, J. A.; Williams, N. X.; Lin, Y.-C.; Franklin, A. D. Uniform and Stable Aerosol Jet Printing of Carbon Nanotube Thin-Film Transistors by Ink Temperature Control. *ACS Appl. Mater. Interfaces* **2020**, *12* (38), 43083−43089.
(107) Tafoya, R. R.; Secor, E. B. Understanding and Mitigating Process Drift in Aerosol Jet Printing. *Flex. Print. Electron.* **2020**, *5* (1), 015009.
(108) Yoo, D.; Mahoney, C. M.; Deneault, J. R.; Grabowski, C.; Austin, D.; Berrigan, J. D.; Glavin, N.; Buskohl, P. R. Mapping Drift in Morphology and Electrical Performance in Aerosol Jet Printing. *Prog. Addit. Manuf.* **2021**, *6*, 257−268.
(109) Salary, R.; Lombardi, J. P.; Samie Tootooni, M.; Donovan, R.; Rao, P. K.; Borgesen, P.; Poliks, M. D. Computational Fluid Dynamics Modeling and Online Monitoring of Aerosol Jet Printing Process. *J. Manuf. Sci. Eng.* **2017**, *139*, 021015.
(110) Mahajan, A.; Frisbie, C. D.; Francis, L. F. Optimization of Aerosol Jet Printing for High-Resolution, High-Aspect Ratio Silver Lines. *ACS Appl. Mater. Interfaces* **2013**, *5* (11), 4856−4864.
(111) Verheecke, W.; Van Dyck, M.; Vogeler, F.; Voet, A.; Valkenaers, H. Optimizing aerosol jet printing of silver interconnects on polyimide film for embedded electronics applications. In *8th International DAAAM Baltic Conference on Industrial Engineering*; DAAAM International: Wien, Austria, 2012; pp 373−379.
(112) Rahul, S. H.; Balasubramanian, K.; Venkatesh, S. Optimizing Inkjet Printing Process to Fabricate Thick Ceramic Coatings. *Ceram. Int.* **2017**, *43* (5), 4513−4519.
(113) Salary, R.; Lombardi, J. P.; Samie Tootooni, M.; Donovan, R.; Rao, P. K.; Borgesen, P.; Poliks, M. D. Computational Fluid Dynamics Modeling and Online Monitoring of Aerosol Jet Printing Process. *J. Manuf. Sci. Eng.* **2017**, *139*, 021015.
(114) Wijshoff, H. Drop Dynamics in the Inkjet Printing Process. *Curr. Opin. Colloid Interface Sci.* **2018**, *36*, 20−27.
(115) Chen, G.; Gu, Y.; Tsang, H.; Hines, D. R.; Das, S. The Effect of Droplet Sizes on Overspray in Aerosol-Jet Printing. *Adv. Eng. Mater.* **2018**, *20* (8), 1701084.
(116) Zhang, H.; Moon, S. K.; Ngo, T. H. 3D Printed Electronics of Non-Contact Ink Writing Techniques: Status and Promise. *Int. J. Precis. Eng. Manuf.-Green Technol.* **2020**, *7* (2), 511−524.
(117) Lim, T.; Yang, J.; Lee, S.; Chung, J.; Hong, D. Deposit Pattern of Inkjet Printed Pico-Liter Droplet. *Int. J. Precis. Eng. Manuf.* **2012**, *13* (6), 827−833.
(118) Yang, Y. J.; Kim, H. C.; Sajid, M.; Kim, S. w.; Aziz, S.; Choi, Y. S.; Choi, K. H. Drop-on-Demand Electrohydrodynamic Printing of High Resolution Conductive Micro Patterns for MEMS Repairing. *Int. J. Precis. Eng. Manuf.* **2018**, *19* (6), 811−819.
(119) Rahman, K.; Khan, A.; Nam, N. M.; Choi, K. H.; Kim, D.-S. Study of Drop-on-Demand Printing through Multi-Step Pulse Voltage. *Int. J. Precis. Eng. Manuf.* **2011**, *12* (4), 663−669.
(120) Tan, H. W.; Tran, T.; Chua, C. K. A Review of Printed Passive Electronic Components through Fully Additive Manufacturing Methods. *Virtual Phys. Prototyp.* **2016**, *11* (4), 271−288.
(121) Smith, M.; Choi, Y. S.; Boughey, C.; Kar-Narayan, S. Controlling and Assessing the Quality of Aerosol Jet Printed Features for Large Area and Flexible Electronics. *Flex. Print. Electron.* **2017**, *2* (1), 015004.
(122) Du, Z.; Lin, Y.; Xing, R.; Cao, X.; Yu, X.; Han, Y. Controlling the Polymer Ink's Rheological Properties and Viscoelasticity to Suppress Satellite Droplets. *Polymer* **2018**, *138*, 75−82.
(123) Jang, D.; Kim, D.; Moon, J. Influence of Fluid Physical Properties on Ink-Jet Printability. *Langmuir* **2009**, *25* (5), 2629−2635.
(124) Derby, B. Inkjet Printing of Functional and Structural Materials: Fluid Property Requirements, Feature Stability, and Resolution. *Annu. Rev. Mater. Res.* **2010**, *40* (1), 395−414.
(125) Son, Y.; Kim, C.; Yang, D. H.; Ahn, D. J. Spreading of an Inkjet Droplet on a Solid Surface with a Controlled Contact Angle at Low Weber and Reynolds Numbers. *Langmuir* **2008**, *24* (6), 2900−2907.
(126) Goth, C.; Putzo, S.; Franke, J. Aerosol Jet Printing on Rapid Prototyping Materials for Fine Pitch Electronic Applications. *In 2011 IEEE 61st Electronic Components and Technology Conference (ECTC)* **2011**, 1211−1216.
(127) Salary, R.; Lombardi, J. P.; Samie Tootooni, M.; Donovan, R.; Rao, P. K.; Borgesen, P.; Poliks, M. D. Computational Fluid Dynamics Modeling and Online Monitoring of Aerosol Jet Printing Process. *J. Manuf. Sci. Eng.* **2017**, *139*, 021015.
(128) Liu, Y.-F.; Tsai, M.-H.; Pai, Y.-F.; Hwang, W.-S. Control of Droplet Formation by Operating Waveform for Inks with Various

https://doi.org/10.1021/acsami.1c04544
ACS Appl. Mater. Interfaces XXXX, XXX, XXX−XXX

Viscosities in Piezoelectric Inkjet Printing. *Appl. Phys. A: Mater. Sci. Process.* **2013**, *111* (2), 509−516.
(129) Shin, P.; Sung, J.; Lee, M. H. Control of Droplet Formation for Low Viscosity Fluid by Double Waveforms Applied to a Piezoelectric Inkjet Nozzle. *Microelectron. Reliab.* **2011**, *51* (4), 797−804.
(130) Yang, L.; Kapur, N.; Wang, Y.; Fiesser, F.; Bierbrauer, F.; Wilson, M. C. T.; Sabey, T.; Bain, C. D. Drop-on-Demand Satellite-Free Drop Formation for Precision Fluid Delivery. *Chem. Eng. Sci.* **2018**, *186*, 102−115.
(131) Gao, Q.; He, Y.; Fu, J.; Qiu, J.; Jin, Y. Fabrication of Shape Controllable Alginate Microparticles Based on Drop-on-Demand Jetting. *J. Sol-Gel Sci. Technol.* **2016**, *77* (3), 610−619.
(132) Mahajan, A.; Frisbie, C. D.; Francis, L. F. Optimization of Aerosol Jet Printing for High-Resolution, High-Aspect Ratio Silver Lines. *ACS Appl. Mater. Interfaces* **2013**, *5* (11), 4856−4864.
(133) Wu, D.; Xu, C. Predictive Modeling of Droplet Formation Processes in Inkjet-Based Bioprinting. *J. Manuf. Sci. Eng.* **2018**, *140*, 101007.
(134) Gan, H. Y.; Shan, X.; Eriksson, T.; Lok, B. K.; Lam, Y. C. Reduction of Droplet Volume by Controlling Actuating Waveforms in Inkjet Printing for Micro-Pattern Formation. *J. Micromech. Microeng.* **2009**, *19* (5), 055010.
(135) van Osch, T. H. J.; Perelaer, J.; de Laat, A. W. M.; Schubert, U. S. Inkjet Printing of Narrow Conductive Tracks on Untreated Polymeric Substrates. *Adv. Mater.* **2008**, *20* (2), 343−345.
(136) Soltman, D.; Subramanian, V. Inkjet-Printed Line Morphologies and Temperature Control of the Coffee Ring Effect. *Langmuir* **2008**, *24* (5), 2224−2231.
(137) Soltman, D.; Subramanian, V. Inkjet-Printed Line Morphologies and Temperature Control of the Coffee Ring Effect. *Langmuir* **2008**, *24* (5), 2224−2231.
(138) Zhao, P.; Huang, J.; Nan, J.; Liu, D.; Meng, F. Laser sintering process optimization of microstrip antenna fabricated by inkjet printing with silver-based MOD ink. *J. Mater. Process. Technol.* **2020**, *275*, 116347.
(139) Sun, J.; Bao, B.; He, M.; Zhou, H.; Song, Y. Recent Advances in Controlling the Depositing Morphologies of Inkjet Droplets. *ACS Appl. Mater. Interfaces* **2015**, *7* (51), 28086−28099.
(140) Polzinger, B.; Schoen, F.; Matic, V.; Keck, J.; Willeck, H.; Eberhardt, W.; Kueck, H. UV-Sintering of Inkjet-Printed Conductive Silver Tracks. In *2011 11th IEEE International Conference on Nanotechnology*, 2011; pp 201−204
(141) Nayak, L.; Mohanty, S.; Nayak, S. K.; Ramadoss, A. A Review on Inkjet Printing of Nanoparticle Inks for Flexible Electronics. *J. Mater. Chem. C* **2019**, *7* (29), 8771−8795.
(142) Yarin, A. L. DROP IMPACT DYNAMICS: Splashing, Spreading, Receding, Bouncing···. *Annu. Rev. Fluid Mech.* **2006**, *38* (1), 159−192.
(143) Jang, D.; Kim, D.; Moon, J. Influence of Fluid Physical Properties on Ink-Jet Printability. *Langmuir* **2009**, *25* (5), 2629−2635.
(144) Martin, G. D.; Hoath, S. D.; Hutchings, I. M. Inkjet Printing - the Physics of Manipulating Liquid Jets and Drops. *J. Phys. Conf. Ser.* **2008**, *105*, 012001.
(145) Derby, B. Inkjet Printing of Functional and Structural Materials: Fluid Property Requirements, Feature Stability, and Resolution. *Annu. Rev. Mater. Res.* **2010**, *40* (1), 395−414.
(146) Brenn, G.; Kolobaric, V. Satellite Droplet Formation by Unstable Binary Drop Collisions. *Phys. Fluids* **2006**, *18* (8), 087101.
(147) Mahonen, A.; Kuusisto, M.; Lindqvist, U.; Nyrhila, R. The Splashing of Ink Drops in CIJ Printing. In *Proceedings of 13th International Conference on Digital Printing Technologies*; Society for Imaging Science and Technology: Springfield, VA, 1997; pp 600−603
(148) Peters, I. R.; Xu, Q.; Jaeger, H. M. Splashing Onset in Dense Suspension Droplets. *Phys. Rev. Lett.* **2013**, *111* (2), 028301.
(149) Can, T. T. T.; Nguyen, T. C.; Choi, W.-S. Patterning of High-Viscosity Silver Paste by an Electrohydrodynamic-Jet Printer for Use in TFT Applications. *Sci. Rep.* **2019**, *9* (1), 1−8.
(150) Jang, D.; Kim, D.; Moon, J. Influence of Fluid Physical Properties on Ink-Jet Printability. *Langmuir* **2009**, *25* (5), 2629−2635.
(151) Zhang, H.; Choi, J. P.; Moon, S. K.; Ngo, T. H. A Hybrid Multi-Objective Optimization of Aerosol Jet Printing Process via Response Surface Methodology. *Addit. Manuf.* **2020**, *33*, 101096.
(152) Seifert, T.; Sowade, E.; Roscher, F.; Wiemer, M.; Gessner, T.; Baumann, R. R. Additive Manufacturing Technologies Compared: Morphology of Deposits of Silver Ink Using Inkjet and Aerosol Jet Printing. *Ind. Eng. Chem. Res.* **2015**, *54* (2), 769−779.
(153) Espera, A. H.; Dizon, J. R. C.; Chen, Q.; Advincula, R. C. 3D-Printing and Advanced Manufacturing for Electronics. *Prog. Addit. Manuf.* **2019**, *4* (3), 245−267.
(154) Onses, M. S.; Sutanto, E.; Ferreira, P. M.; Alleyne, A. G.; Rogers, J. A. Mechanisms, capabilities, and applications of high-resolution electrohydrodynamic jet printing. *Small* **2015**, *11* (34), 4237−4266.
(155) Xu, Y.; Wu, X.; Guo, X.; Kong, B.; Zhang, M.; Qian, X.; Mi, S.; Sun, W. The Boom in 3D-Printed Sensor Technology. *Sensors* **2017**, *17* (5), 1166.
(156) Eggenhuisen, T. M.; Galagan, Y.; Biezemans, A. F. K. V.; Slaats, T. M. W. L.; Voorthuijzen, W. P.; Kommeren, S.; Shanmugam, S.; Teunissen, J. P.; Hadipour, A.; Verhees, W. J. H.; Veenstra, S. C.; Coenen, M. J. J.; Gilot, J.; Andriessen, R.; Groen, W. A. High Efficiency, Fully Inkjet Printed Organic Solar Cells with Freedom of Design. *J. Mater. Chem. A* **2015**, *3* (14), 7255−7262.
(157) Karunakaran, S. K.; Arumugam, G. M.; Yang, W.; Ge, S.; Khan, S. N.; Lin, X.; Yang, G. Recent Progress in Inkjet-Printed Solar Cells. *J. Mater. Chem. A* **2019**, *7* (23), 13873−13902.
(158) Lee, S.-H.; Cho, Y.-J. Characterization of Silver Inkjet Overlap-Printing through Cohesion and Adhesion. *J. Electr. Eng. Technol.* **2012**, *7* (1), 91−96.
(159) Smith, M.; Choi, Y. S.; Boughey, C.; Kar-Narayan, S. Controlling and Assessing the Quality of Aerosol Jet Printed Features for Large Area and Flexible Electronics. *Flex. Print. Electron.* **2017**, *2* (1), 015004.
(160) Lall, P.; Abrol, A.; Kothari, N.; Leever, B.; Miller, S. Process Capability of Aerosol-Jet Additive Processes for Long-Runs Up to 10-h. *J. Electron. Packag.* **2020**, *142* (4), 041003.
(161) Lombardi, J. P.; Salary, R.; Weerawarne, D. L.; Rao, P. K.; Poliks, M. D. Image-Based Closed-Loop Control of Aerosol Jet Printing Using Classical Control Methods. *J. Manuf. Sci. Eng.* **2019**, *141* (7), 071011.
(162) Tafoya, R. R.; Cook, A. W.; Kaehr, B.; Downing, J. R.; Hersam, M. C.; Secor, E. B. Real-Time Optical Process Monitoring for Structure and Property Control of Aerosol Jet Printed Functional Materials. *Adv. Mater. Technol.* **2020**, *5* (12), 2000781.
(163) Secor, E. B. Guided Ink and Process Design for Aerosol Jet Printing Based on Annular Drying Effects. *Flex. Print. Electron.* **2018**, *3* (3), 035007.
(164) Gu, Y.; Gutierrez, D.; Das, S.; Hines, D. R. Inkwells for On-Demand Deposition Rate Measurement in Aerosol-Jet Based 3D Printing. *J. Micromech. Microeng.* **2017**, *27* (9), 097001.
(165) Wadhwa, A. Run-Time Ink Stability in Pneumatic Aerosol Jet Printing Using a Split Stream Solvent Add Back System. *Thesis*, Rochester Institute of Technology, Rochester, NY, 2015.
(166) Fromm, J. E. Numerical calculation of the fluid dynamics of drop-on-demand jets. *IBM J. Res. Dev.* **1984**, *28* (3), 322−333.
(167) Güngör, G. L.; Kara, A.; Gardini, D.; Blosi, M.; Dondi, M.; Zanelli, C. Ink-Jet Printability of Aqueous Ceramic Inks for Digital Decoration of Ceramic Tiles. *Dyes Pigm.* **2016**, *127*, 148−154.
(168) Reis, N.; Derby, B. Ink Jet Deposition of Ceramic Suspensions: Modeling and Experiments of Droplet Formation. *MRS Online Proc. Libr.* **2000**, *624* (1), 65−70.
(169) Derby, B. Inkjet Printing of Functional and Structural Materials: Fluid Property Requirements, Feature Stability, and Resolution. *Annu. Rev. Mater. Res.* **2010**, *40* (1), 395−414.

https://doi.org/10.1021/acsami.1c04544
ACS Appl. Mater. Interfaces XXXX, XXX, XXX−XXX

(170) Jang, D.; Kim, D.; Moon, J. Influence of Fluid Physical Properties on Ink-Jet Printability. *Langmuir* **2009**, *25* (5), 2629−2635.
(171) Jo, B. W.; Lee, A.; Ahn, K. H.; Lee, S. J. Evaluation of Jet Performance in Drop-on-Demand (DOD) Inkjet Printing. *Korean J. Chem. Eng.* **2009**, *26* (2), 339−348.
(172) Seerden, K. A. M.; Reis, N.; Evans, J. R. G.; Grant, P. S.; Halloran, J. W.; Derby, B. Ink-Jet Printing of Wax-Based Alumina Suspensions. *J. Am. Ceram. Soc.* **2001**, *84* (11), 2514−2520.
(173) Wu, H.-C.; Hwang, W.-S.; Lin, H.-J. Development of a Three-Dimensional Simulation System for Micro-Inkjet and Its Experimental Verification. *Mater. Sci. Eng., A* **2004**, *373* (1), 268−278.
(174) de Gans, B.-J.; Duineveld, P. C.; Schubert, U. S. Inkjet Printing of Polymers: State of the Art and Future Developments. *Adv. Mater.* **2004**, *16* (3), 203−213.
(175) Szczech, J.B.; Megaridis, C.M.; Gamota, D.R.; Zhang, J. Fine-Line Conductor Manufacturing Using Drop-on Demand PZT Printing Technology. *IEEE Trans. Electron. Packag. Manuf.* **2002**, *25* (1), 26−33.
(176) Perelaer, J.; Smith, P. J.; Wijnen, M. M. P.; van den Bosch, E.; Eckardt, R.; Ketelaars, P. H. J. M.; Schubert, U. S. Droplet Tailoring Using Evaporative Inkjet Printing. *Macromol. Chem. Phys.* **2009**, *210* (5), 387−393.
(177) Shin, P.; Sung, J.; Lee, M. H. Control of Droplet Formation for Low Viscosity Fluid by Double Waveforms Applied to a Piezoelectric Inkjet Nozzle. *Microelectron. Reliab.* **2011**, *51* (4), 797−804.
(178) Son, Y.; Kim, C.; Yang, D. H.; Ahn, D. J. Spreading of an Inkjet Droplet on a Solid Surface with a Controlled Contact Angle at Low Weber and Reynolds Numbers. *Langmuir* **2008**, *24* (6), 2900−2907.
(179) Gan, H. Y.; Shan, X.; Eriksson, T.; Lok, B. K.; Lam, Y. C. Reduction of Droplet Volume by Controlling Actuating Waveforms in Inkjet Printing for Micro-Pattern Formation. *J. Micromech. Microeng.* **2009**, *19* (5), 055010.
(180) Dong, H.; Carr, W. W.; Morris, J. F. An Experimental Study of Drop-on-Demand Drop Formation. *Phys. Fluids* **2006**, *18* (7), 072102.
(181) Duineveld, P. C. The Stability of Ink-Jet Printed Lines of Liquid with Zero Receding Contact Angle on a Homogeneous Substrate. *J. Fluid Mech.* **2003**, *477*, 175−200.
(182) Davis, S. H. Moving contact lines and rivulet instabilities. Part 1. The static rivulet. *J. Fluid Mech.* **1980**, *98* (2), 225−242.
(183) Schiaffino, S.; Sonin, A. A. Formation and Stability of Liquid and Molten Beads on a Solid Surface. *J. Fluid Mech.* **1997**, *343*, 95−110.
(184) Stringer, J.; Derby, B. Limits to Feature Size and Resolution in Ink Jet Printing. *J. Eur. Ceram. Soc.* **2009**, *29* (5), 913−918.
(185) Chen, F. Development of Drop-on-Demand Sample Injection System by Inkjet Technology and Its Application to Analytical Chemistry. *Thesis*, Tokyo Metropolitan University, Tokyo, 2014.
(186) Wu, J.-T.; Hsu, S. L.-C.; Tsai, M.-H.; Hwang, W.-S. Direct Inkjet Printing of Silver Nitrate/Poly(*N* -Vinyl-2-Pyrrolidone) Inks to Fabricate Silver Conductive Lines. *J. Phys. Chem. C* **2010**, *114* (10), 4659−4662.
(187) Wang, C.; Hopkins, S. C.; Tomov, R. I.; Kumar, R. V.; Glowacki, B. A. Optimisation of CGO Suspensions for Inkjet-Printed SOFC Electrolytes. *J. Eur. Ceram. Soc.* **2012**, *32* (10), 2317−2324.
(188) Gao, Q.; He, Y.; Fu, J.; Qiu, J.; Jin, Y. Fabrication of Shape Controllable Alginate Microparticles Based on Drop-on-Demand Jetting. *J. Sol-Gel Sci. Technol.* **2016**, *77* (3), 610−619.
(189) Herran, C. L.; Huang, Y. Alginate Microsphere Fabrication Using Bipolar Wave-Based Drop-on-Demand Jetting. *J. Manuf. Process.* **2012**, *14* (2), 98−106.
(190) Binder, S.; Glatthaar, M.; Rädlein, E. Analytical Investigation of Aerosol Jet Printing. *Aerosol Sci. Technol.* **2014**, *48* (9), 924−929.
(191) Nguyen, H. A. D.; Lee, J.; Kim, C. H.; Shin, K.-H.; Lee, D. An Approach for Controlling Printed Line-Width in High Resolution Roll-to-Roll Gravure Printing. *J. Micromech. Microeng.* **2013**, *23* (9), 095010.
(192) van den Berg, A. M. J.; de Laat, A. W. M.; Smith, P. J.; Perelaer, J.; Schubert, U. S. Geometric Control of Inkjet Printed Features Using a Gelating Polymer. *J. Mater. Chem.* **2007**, *17* (7), 677−683.
(193) Chouiki, M.; Schoeftner, R. Inkjet Printing of Inorganic Sol-Gel Ink and Control of the Geometrical Characteristics. *J. Sol-Gel Sci. Technol.* **2011**, *58* (1), 91−95.
(194) Feng, J. Q. A Computational Study of Particle Deposition Patterns from a Circular Laminar Jet. *J. Appl. Fluid Mech.* **2017**, *10* (4), 1001−1012.
(195) Chen, G.; Gu, Y.; Tsang, H.; Hines, D. R.; Das, S. The Effect of Droplet Sizes on Overspray in Aerosol-Jet Printing. *Adv. Eng. Mater.* **2018**, *20* (8), 1701084.
(196) Lall, P.; Kothari, N.; Abrol, A.; Suhling, J.; Ahmed, S.; Leever, B.; Miller, S. Effect of Process Parameters on the Long-Run Print Consistency and Material Properties of Additively Printed Electronics. In *2019 IEEE 69th Electronic Components and Technology Conference (ECTC)*; IEEE: Piscataway, NJ, 2019; pp 1347−1358.
(197) Lombardi, J. P., III; Salary, R.; Weerawarne, D. L.; Rao, P. K.; Poliks, M. D. Image-Based Closed-Loop Control of Aerosol Jet Printing Using Classical Control Methods. *J. Manuf. Sci. Eng.* **2019**, *141*, 071011.
(198) Salary, R.; Lombardi, J. P.; Rao, P. K.; Poliks, M. D. Online Monitoring of Functional Electrical Properties in Aerosol Jet Printing Additive Manufacturing Process Using Shape-From-Shading Image Analysis. *J. Manuf. Sci. Eng.* **2017**, *139*, 101010.
(199) Lee, J.; Oh, S. J.; An, S. H.; Kim, W.-D.; Kim, S.-H. Machine Learning-Based Design Strategy for 3D Printable Bioink: Elastic Modulus and Yield Stress Determine Printability. *Biofabrication* **2020**, *12* (3), 035018.
(200) Menon, A.; Póczos, B.; Feinberg, A. W.; Washburn, N. R. Optimization of Silicone 3D Printing with Hierarchical Machine Learning. *3D Print. Addit. Manuf.* **2019**, *6* (4), 181−189.
(201) Shi, J.; Song, J.; Song, B.; Lu, W. F. Multi-Objective Optimization Design through Machine Learning for Drop-on-Demand Bioprinting. *Engineering* **2019**, *5* (3), 586−593.
(202) Ruberu, K.; Senadeera, M.; Rana, S.; Gupta, S.; Chung, J.; Yue, Z.; Venkatesh, S.; Wallace, G. Coupling Machine Learning with 3D Bioprinting to Fast Track Optimisation of Extrusion Printing. *Appl. Mater. Today* **2021**, *22*, 100914.
(203) Uzun-Per, M.; Gillispie, G. J.; Tavolara, T. E.; Yoo, J. J.; Atala, A.; Gurcan, M. N.; Lee, S. J.; Niazi, M. K. K. Automated Image Analysis Methodologies to Compute Bioink Printability. *Adv. Eng. Mater.* **2021**, *23* (4), 2000900.
(204) Huang, J.; Segura, L. J.; Wang, T.; Zhao, G.; Sun, H.; Zhou, C. Unsupervised Learning for the Droplet Evolution Prediction and Process Dynamics Understanding in Inkjet Printing. *Addit. Manuf.* **2020**, *35*, 101197.
(205) Zhang, H.; Moon, S. K.; Ngo, T. H. Hybrid Machine Learning Method to Determine the Optimal Operating Process Window in Aerosol Jet 3D Printing. *ACS Appl. Mater. Interfaces* **2019**, *11* (19), 17994−18003.
(206) Lies, B. T.; Cai, Y.; Spahr, E.; Lin, K.; Qin, H. Machine Vision Assisted Micro-Filament Detection for Real-Time Monitoring of Electrohydrodynamic Inkjet Printing. *Procedia Manuf.* **2018**, *26*, 29−39.
(207) Wang, T.; Zhou, C.; Xu, W. Online Droplet Monitoring in Inkjet 3D Printing Using Catadioptric Stereo System. *IISE Trans.* **2019**, *51* (2), 153−167.
(208) Segura, L. J.; Wang, T.; Zhou, C.; Sun, H. Online Droplet Anomaly Detection from Streaming Videos in Inkjet Printing. *Addit. Manuf.* **2021**, *38*, 101835.
(209) Salary, R.; Lombardi, J. P.; Rao, P. K.; Poliks, M. D. Online Monitoring of Functional Electrical Properties in Aerosol Jet Printing Additive Manufacturing Process Using Shape-From-Shading Image Analysis. *J. Manuf. Sci. Eng.* **2017**, *139* (10), 101010.

https://doi.org/10.1021/acsami.1c04544
ACS Appl. Mater. Interfaces XXXX, XXX, XXX−XXX

(210) Li, Y.; Sun, H.; Deng, X.; Zhang, C.; Wang, H.-P.; Jin, R. Manufacturing Quality Prediction Using Smooth Spatial Variable Selection Estimator with Applications in Aerosol Jet® Printed Electronics Manufacturing. *IISE Trans.* **2020**, *52* (3), 321−333.
(211) Yan, Y.; Yang, Q.; Maize, K.; Allebach, J. P.; Shakouri, A.; Chiu, G. T. Image-Based Non-Contact Conductivity Prediction for Inkjet Printed Electrodes. *NIP Digit. Fabr. Conf.* **2019**, 152−157.
(212) Wang, T.; Kwok, T.-H.; Zhou, C.; Vader, S. In-Situ Droplet Inspection and Closed-Loop Control System Using Machine Learning for Liquid Metal Jet Printing. *J. Manuf. Syst.* **2018**, *47*, 83−92.
(213) Shi, J.; Wu, B.; Song, B.; Song, J.; Li, S.; Trau, D.; Lu, W. F. Learning-Based Cell Injection Control for Precise Drop-on-Demand Cell Printing. *Ann. Biomed. Eng.* **2018**, *46* (9), 1267−1279.
(214) Ball, A. K.; Das, R.; Roy, S. S.; Kisku, D. R.; Murmu, N. C. Modeling of EHD Inkjet Printing Performance Using Soft Computing-Based Approaches. *Soft Comput.* **2020**, *24* (1), 571−589.
(215) Tourloukis, G.; Stoyanov, S.; Tilford, T.; Bailey, C. Predictive Modelling for 3D Inkjet Printing Processes. *2016 39th Int. Spring Semin. Electron. Technol.* **2016**, *6*, 257−262.
(216) Inyang-Udoh, U.; Mishra, S. A Learning-based Approach to Modeling and Control of Inkjet 3D Printing. *In 2020 American Control Conference* **2020**, 460−466.
(217) He, H.; Yang, Y.; Pan, Y. Machine Learning for Continuous Liquid Interface Production: Printing Speed Modelling. *J. Manuf. Syst.* **2019**, *50*, 236−246.
(218) Chang, Y.-H. Process Monitoring, Modeling, and Quality Assessment for Printed Electronics with Aerosol Jet Printing Technology. *Thesis*, Georgia Tech, Atlanta, GA, 2017.
(219) Zhang, H.; Choi, J. P.; Moon, S. K.; Ngo, T. H. A Multi-Objective Optimization Framework for Aerosol Jet Customized Line Width Printing via Small Data Set and Prediction Uncertainty. *J. Mater. Process. Technol.* **2020**, *285*, 116779.
(220) Yuan, J.; Wang, K.; Yu, T.; Fang, M. Reliable Multi-Objective Optimization of High-Speed WEDM Process Based on Gaussian Process Regression. *Int. J. Mach. Tools Manuf.* **2008**, *48* (1), 47−60.
(221) Luo, L.; Yao, Y.; Gao, F. Bayesian Improved Model Migration Methodology for Fast Process Modeling by Incorporating Prior Information. *Chem. Eng. Sci.* **2015**, *134*, 23−35.
(222) Lu, J.; Yao, Y.; Gao, F. Model Migration for Development of a New Process Model. *Ind. Eng. Chem. Res.* **2009**, *48* (21), 9603−9610.
(223) Zhang, H.; Choi, J. P.; Moon, S. K.; Ngo, T. H. A Knowledge Transfer Framework to Support Rapid Process Modeling in Aerosol Jet Printing. *Adv. Eng. Inform.* **2021**, *48*, 101264.
(224) Tafoya, R. R.; Cook, A. W.; Kaehr, B.; Downing, J. R.; Hersam, M. C.; Secor, E. B. Real-Time Optical Process Monitoring for Structure and Property Control of Aerosol Jet Printed Functional Materials. *Adv. Mater. Technol.* **2020**, *5* (12), 2000781.
(225) Salary, R.; Lombardi, J. P.; Weerawarne, D. L.; Tootooni, M. S.; Rao, P. K.; Poliks, M. D. A Sparse Representation Classification Approach for Near Real-Time, Physics-Based Functional Monitoring of Aerosol Jet-Fabricated Electronics. *J. Manuf. Sci. Eng.* **2020**, *142* (8), 081007.
(226) Kien Nguyen, T.; Nguyen, V. D.; Seong, B.; Hoang, N.; Park, J.; Byun, D. Control and Improvement of Jet Stability by Monitoring Liquid Meniscus in Electrospray and Electrohydrodynamic Jet. *J. Aerosol Sci.* **2014**, *71*, 29−39.
(227) Wang, A.; Wang, T.; Zhou, C.; Xu, W. LuBan: Low-Cost and In-Situ Droplet Micro-Sensing for Inkjet 3D Printing Quality Assurance. In *Proceedings of the 15th ACM Conference on Embedded Network Sensor Systems SenSys '17*; Association for Computing Machinery: New York, NY, 2017; pp 1−14.
(228) Lies, B. T.; Spahr, E.; Lin, K.; Qin, H. Machine Vision Assisted Micro-Filament Detection for Real-Time Monitoring of Electro-hydrodynamic Inkjet Printing. *Procedia Manuf.* **2018**, *26*, 29−39.
(229) Li, Y.; Sun, H.; Deng, X.; Zhang, C.; Wang, H.-P.; Jin, R. Manufacturing Quality Prediction Using Smooth Spatial Variable Selection Estimator with Applications in Aerosol Jet® Printed Electronics Manufacturing. *IISE Trans.* **2020**, *52* (3), 321−333.
(230) Kwon, K.-S. Speed Measurement of Ink Droplet by Using Edge Detection Techniques. *Measurement* **2009**, *42* (1), 44−50.
(231) Formentin, S.; van Heusden, K.; Karimi, A. A Comparison of Model-Based and Data-Driven Controller Tuning. *Int. J. Adapt. Control Signal Process.* **2014**, *28* (10), 882−897.
(232) Hou, Z.-S.; Wang, Z. From Model-Based Control to Data-Driven Control: Survey, Classification and Perspective. *Inf. Sci.* **2013**, *235*, 3−35.
(233) Fukuda, K.; Sekine, T.; Kumaki, D.; Tokito, S. Profile Control of Inkjet Printed Silver Electrodes and Their Application to Organic Transistors. *ACS Appl. Mater. Interfaces* **2013**, *5* (9), 3916−3920.

https://doi.org/10.1021/acsami.1c04544
ACS Appl. Mater. Interfaces XXXX, XXX, XXX−XXX